ChemPubSoc Europe

DOI: 10.1002/chem.201403467

CHEMISTRY
A European Journal
Full Paper

Self-Assembly

Kinetico-Mechanistic Insights on the Assembling Dynamics of Allyl-Cornered Metallacycles: The Pt–N_{py} Bond is the Keystone

Inmaculada Angurell,[a] Montserrat Ferrer,*[a] Albert Gutiérrez,[a] Manuel Martínez,*[a] Mercè Rocamora,[a] Laura Rodríguez,[a] Oriol Rossell,[a] Yvonne Lorenz,[b] and Marianne Engeser[b]

Abstract: The square-like homo- and heterometallamacrocycles $[\{Pd(\eta^3\text{-2-Me-}C_3H_4)(\mathbf{L}^n)\}_2\}_2\{M(dppp)\}_2](CF_3SO_3)_6$ (dppp = 1,3-bis(diphenylphosphino)propane) and $[\{Pd(\eta^3\text{-2-Me-}C_3H_4)(\mathbf{L}^1)\}_2\}_2\{M(PPh_3)_2\}_2](CF_3SO_3)_6$ [py = pyridine, M = Pd, Pt, $\mathbf{L}^n$ = 4-PPh_2py ($\mathbf{L}^1$), 4-$C_6F_4PPh_2$py ($\mathbf{L}^2$)] containing allyl corners were synthesised by antisymbiotic self-assembly of the different palladium and platinum metallic corners and the ambidentate N,P ligands. All the synthesised assemblies displayed a complex dynamic behaviour in solution, the rate of which is found to be dependent on the electronic and/or steric nature of the different building blocks. A kinetico-mechanistic study by NMR line shape analysis of the dynamics of some of these assemblies was undertaken in order to determine the corresponding thermal activation parameters. Both an enhanced thermodynamic stability and slower dynamics were observed for platinum-pyridine-containing species when compared with their palladium analogues. Time-dependent NMR spectroscopy in combination with ESI mass spectrometry was used to study the exchange between the assemblies and their building blocks, as well as that occurring between different metallamacrocycles. Preliminary studies were carried out on the activity of some of the metallamacrocyclic compounds as catalytic precursors in the allylic substitution reaction, and the results compared with that of the monometallic allylic corner $[Pd(\eta^3\text{-2-Me-}C_3H_4)(\mathbf{L}^1)_2]^+$.

Introduction

Since the dawn of supramolecular coordination chemistry in the 1980s, an overwhelming number of discrete metallasupramolecular architectures with different combinations of metal centres and ligands has been synthesised and characterised.[1] Although the formation of complex and aesthetically pleasing structures has been a goal by itself in many cases, the potential of self-assembled structures originates in the derived functions of the species produced. In this respect, functionalisation of these architectures, which is possible by employing function-specific ligands and/or metal centres in the assembly process, should produce molecules having a potential use as catalysts, sensors or in material sciences.[1f,l,2]

[a] Dr. I. Angurell, Dr. M. Ferrer, Dr. A. Gutiérrez, Prof. M. Martínez, Dr. M. Rocamora, Dr. L. Rodríguez, Prof. O. Rossell
Departament de Quimica Inorgànica
Universitat de Barcelona
Martí i Franquès 1-11, 08028 Barcelona (Spain)
Fax: (+34) 93 4907725
E-mail: montse.ferrer@qi.ub.es
manel.martinez@qi.ub.es

[b] Dipl.-Chem. Y. Lorenz, Dr. M. Engeser
Kekulé-Institut für Organische Chemie und Biochemie
Universität Bonn
Gerhard-Domagk-Str.1
53121 Bonn (Germany)

Supporting information for this article is available on the WWW under http://dx.doi.org/10.1002/chem.201403467.

Even though the use of supramolecules as reactors has provided a significant number of amazing examples of activity and selectivity,[3] an alternative approach by designing new functional self-assembled supramolecular metallamacrocycles is also possible; the final purpose being their direct participation in selected catalytic processes.[4] In particular, and given the fact that the majority of the assembled complexes reported so far have coordinatively inert metal centres, the incorporation of weakly coordinating ligands, such as olefins, seems to be a good strategy to preclude the destruction of the supramolecular species during the catalytic transformations.

With this alternative strategy in mind, we have recently described[5] the incorporation of allyl-palladium building blocks such as $\{Pd(\eta^3\text{-2-Me-}C_3H_4)\}^+$, into well-defined, self-assembled homo- and heterometalla architectures. In these, the typical diphosphane or diamine capping ligands have been substituted in part by the 2-Me-C_3H_4 allyl group. It is known that allyl-palladium moieties have a potential utility in processes that form new C–C or carbon–heteroatom bonds,[6] either as precursors of the catalytic species or as intermediates. These include allylic substitutions[7] and hydrovinylation reactions[8] that could be incorporated to the metallamacrocyclic reactivity. Surprisingly, despite these obvious reasons for the interest in these macrocyclic architectures, little work in the field has been carried out.

In our preliminary study[5] we found that the obtained allyl-palladium metallamacrocycles, $[\{Pd(\eta^3\text{-2-Me-}C_3H_4)(PPh_2py)_2\}_2\{M(dppp)\}_2](CF_3SO_3)_6$ (dppp = 1,3-bis(diphenylphosphino)propane,

M = Pd, Pt), featured a rather uncommon dynamic behaviour in solution that implied, in the case of the platinum-containing species, a remarkable lability of the usually inert Pt^{II} square-planar centres. Although the dynamic nature of coordination bonds in self-assembly is widely recognised as a keystone of the nature of supramolecular architectures, only few studies that characterise in a systematic and quantitative way such exchanges in this kind of species have been reported.[9] It is clear that a good knowledge of the general solution behaviour, as well as detailed thermodynamic and/or kinetic data for the molecular self-assembled systems, become especially important when rationalising their application in different functions, such as molecular recognition or catalytic processes among others.

In our previous communication[5] we described the selective self-assembly of the dppp derivatives **1a** and **1b**, the allyl-palladium metallic block **c**, and the heteroditopic linker $\mathbf{L^1}$ to produce square like metallamacrocycles displaying two different metal corners $\mathbf{1aL^1c}$ and $\mathbf{1bL^1c}$ (Scheme 1).

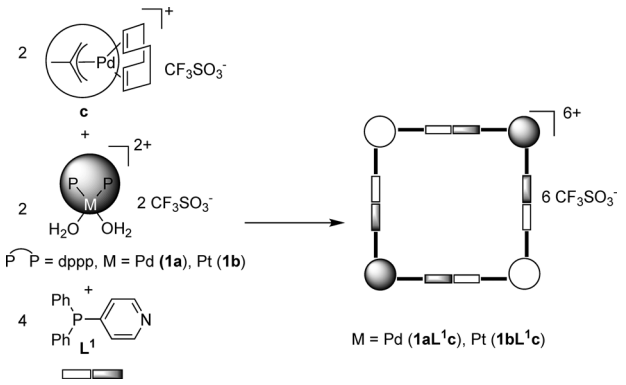

Scheme 1. Schematic representation of the self-assembly of the dppp derivatives **1a** and **1b**, the allyl-palladium building block **c** and the linker $\mathbf{L^1}$.

In that paper, we provided a detailed characterisation of these species, including X-ray crystal structure determination, fluxional behaviour in different solvents and a kinetico-mechanistic study of the non-rigidity of the $\mathbf{1aL^1c}$ compound. The obtained thermal activation parameters were indicative of an associatively activated exchange process that involved the whole metallamacrocycle and some of its fragments. This exchange mechanism is in contrast with that based on the rotation of the pyridine moiety of the ligand $\mathbf{L^1}$, postulated by several authors.[9b,10]

In the present report, we expand the scope of the described methodology to diverse homo- and heterometalla macrocyclic structures with allyl-palladium $\{Pd(\eta^3\text{-}2\text{-}Me\text{-}C_3H_4)\}$ subunits. In these structures, the basicity of the phosphane ligands at the corners and/or the size of the resulting metallacycles have been carefully tuned. The different dynamic processes involved in the synthesis and stability of the prepared species have been looked into, and a preliminary study about the activity of some of these compounds as catalysts in the allylic alkylation process has been undertaken.

Results and Discussion

Synthesis and characterisation of the ligand 4-$PPh_2C_6F_4py$ ($\mathbf{L^2}$) (py = pyridine)

With the aim of obtaining larger metallamacrocycles than $\mathbf{1aL^1c}$ and $\mathbf{1bL^1c}$ (Scheme 1), the new ambidentate ligand $\mathbf{L^2}$, that is, 4-(4-diphenylphosphino)-tetrafluorophenylpyridine, was synthesised by lithiation of the previously described[11] 4-bromo-tetrafluorophenylpyridine by using *n*BuLi (1.6 M in hexane) in a thf solution at −78 °C, followed by the addition of diphenylchlorophosphane at the same temperature (Scheme 2). A white crystalline solid was obtained, which showed spectroscopic, mass spectrometric and analysis data consistent with the proposed structure (see the Experimental Section).

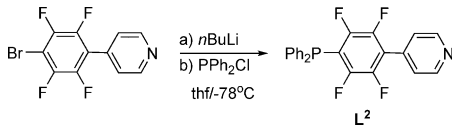

Scheme 2. Synthesis of ligand $\mathbf{L^2}$.

Synthesis and characterisation of the metallamacrocycles

As indicated above, our interest was centred on widening our study of the metallamacrocycles depicted in Scheme 1 by tuning the basicity and/or size of the different building blocks in order to better understand the observed exchange process. As a first option, two PPh_3 ligands were used as ancillary ligands in the non-organometallic corner instead of the chelating ligand dppp. For the synthesis of a homometallic derivative $[\{Pd(\eta^3\text{-}2\text{-}Me\text{-}C_3H_4)(PPh_2py)_2\}_2\{Pd(PPh_3)\}_2](CF_3SO_3)_6$ ($\mathbf{2aL^1c}$), the self-assembly reaction (Scheme 3, left) was performed under the same conditions than those already used for the synthesis of $\mathbf{1aL^1c}$ and $\mathbf{1bL^1c}$.[5] Mixing $[Pd(\eta^3\text{-}2\text{-}Me\text{-}C_3H_4)(cod)](CF_3SO_3)$ (**c**, cod = 1,5-cyclooctadiene), $[Pd(H_2O)_2(PPh_3)_2](CF_3SO_3)_2$ (**2a**) and 4-PPh_2py ($\mathbf{L^1}$) in a molar ratio of 1:1:2 in CH_2Cl_2 at room temperature produced the targeted metallamacrocycle $\mathbf{2aL^1c}$ as a white solid in good yield. Alternatively, the same macrocycle, that is, $\mathbf{2aL^1c}$, can be obtained by reaction of the preformed $[Pd(\eta^3\text{-}2\text{-}Me\text{-}C_3H_4)(4\text{-}PPh_2py)_2](CF_3SO_3)$ ($\mathbf{L^1c}$) with the bis(triphenylphosphane) corner block **2a** under the same conditions of solvent and temperature (Scheme 3, right).

For the synthesis of the analogous heterometallamacrocycle $\mathbf{2bL^1c}$, namely $[\{Pd(\eta^3\text{-}2\text{-}Me\text{-}C_3H_4)(PPh_2py)_2\}_2\{Pt(PPh_3)\}_2](CF_3SO_3)_6$, a new strategy had to be used because the platinum acceptor unit $[Pt(H_2O)_2(PPh_3)_2](CF_3SO_3)_2$ (**2b**) could not be isolated in solid state. Unlike for the palladium compound *cis*-$[PdCl_2(PPh_3)_2]$, treatment of *cis*-$[PtCl_2(PPh_3)_2]$ with silver triflate resulted in the formation of unidentified silver phosphane derivatives; therefore, the acceptor corner $\{Pt(PPh_3)_2\}^{2+}$ (**2b**) was generated in situ. Thus, equimolar quantities of the preformed allyl palladium donor $[Pd(\eta^3\text{-}2\text{-}Me\text{-}C_3H_4)(4\text{-}PPh_2py)_2](CF_3SO_3)$ ($\mathbf{L^1c}$) and the precursor *cis*-$[PtCl_2(PPh_3)_2]$ were mixed in dichloro-

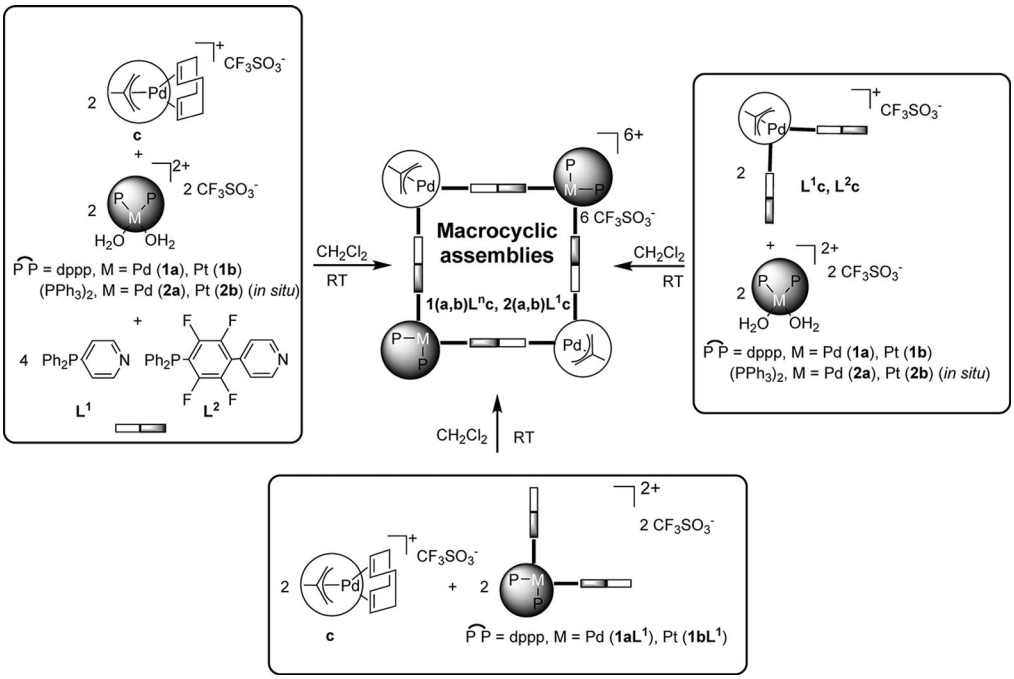

Scheme 3. Self-assembly pathways for the generation of the different metallamacrocycles.

methane at room temperature and, after several minutes, two equivalents of solid $AgCF_3SO_3$ were added with constant stirring. After two hours and subsequent work up the new macrocycle **2bL^{1}c** was obtained as a yellow powder in good yield. Similarly to the ones previously described for the macrocycles **1aL^{1}c** and **1bL^{1}c**,[5] the $^{31}P\{^1H\}$ NMR spectra of the new compounds **2aL^{1}c** and **2bL^{1}c** showed two singlets that can be assigned to the P atoms of the PPh_3 and 4-PPh_2py ligands, respectively. As expected, ^{195}Pt satellites ($^1J(P,Pt) = 3323$ Hz) associated with the PPh_3 signals were found for the heterometallic Pd/Pt macrocycle **2bL^{1}c**. The ^1H NMR spectra were found to be solvent- and temperature-dependent; in $CDCl_3$ and at 298 K the ^1H NMR spectra of **2aL^{1}c** and **2bL^{1}c** display rather broad signals that sharpen and/or split on lowering the temperature. As an example, compound $[\{Pd(\eta^3\text{-}2\text{-}Me\text{-}C_3H_4)(PPh_2py)_2\}_2\{Pd(PPh_3)\}_2](CF_3SO_3)_6$ (**2aL^{1}c**), shows a broad single resonance at 298 K assigned to the α-pyridine protons, which splits into two different peaks at approximately 240 K (Figure 1, top). The observed low-temperature NMR pattern resembles the one found for the related dppp derivative **1aL^{1}c** at 298 K (Figure 1, middle). On the other hand, the ^1H NMR spectrum in $CDCl_3$ of the **2bL^{1}c** analogue shows different α and α′ pyridine proton broad signals at 298 K (Figure 1, bottom), which fully sharpen at approximately 280 K. However, in the more coordinating medium acetone, only one set of sharp signals was observed for the pyridine protons at room temperature (Figures S1 and S2 in the Supporting Information). Thus, variable-temperature (VT)-NMR studies clearly indicate that the palladium macrocycle **2aL^{1}c** shows faster dynamics than the Pt–N bond-containing, heterometallic analogue **2bL^{1}c**. This is in agreement with the relative inertness of Pt^{II} complexes, as shown in many nucleophilic substitution processes.[12]

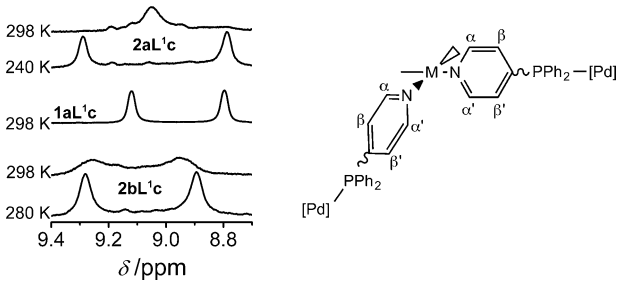

Figure 1. Temperature-dependent ^1H NMR spectra of the α pyridine region for the different metallamacrocycles.

The formation of the PPh_3-containing metallamacrocycles, **2aL^{1}c** and **2bL^{1}c** was further supported by ESI Fourier transform ion cyclotron resonance (FTICR) mass spectrometry as shown in the Supporting Information (Figures S3 and S4). The mass spectrum of **2aL^{1}c** displays a peak at $m/z = 1617.2$ corresponding to the doubly charged species $[\mathbf{2aL^1c}\text{-}2(CF_3SO_3)]^{2+}$, which appears superimposed with that of the mono-charged $[Pd_2(\eta^3\text{-}2\text{-}Me\text{-}C_3H_4)(PPh_3)_2(4\text{-}PPh_2py)_2(CF_3SO_3)_2]^+$ fragment formed by fragmentation of the macrocyclic architecture. For the platinum-containing compound **2bL^{1}c**, the peaks corresponding to the loss of two ($m/z = 1706.2$) and three ($m/z = 1087.5$) triflate anions from the compound are observed, as well as a signal at $m/z = 2324.3$ that corresponds to the triply charged aggregation species $[(\mathbf{2aL^1c})_2\text{-}3(CF_3SO_3)]^{3+}$, (arising from the interaction of two metallamacrocycles and the loss of three triflate anions).[13] In both spectra, additional signals were observed, which are due to fragmentation processes occurring in the electrospray source and which are in full accordance with the structure of the macrocycles.

Once the changes in the phosphane capping ligand had been studied, the effect on the solution dynamics of increasing the macrocyclic size by changing the connecting ambidentate ligand was pursued. The new heteroditopic ligand bearing one tetrafluorobenzene group between the pyridine and the phosphorus atom, 4-$PPh_2C_6F_4py$ (**L²**) was utilised, whereas the basicity and bite angle on the phosphane-containing corner was maintained as in the ligand dppp. Additionally, apart from allowing the creation of bigger assemblies, ligand **L²** has different electronic characteristics than its related counterpart **L¹**. The introduction of a perfluorinated group next to the pyridine ring produces a decrease of the basicity of the N_{py} atom, which has to be considered when discussing the dynamics of the system.

Ligand **L²** efficiently self-assembles with $[M(H_2O)_2(dppp)]^{2+}$ [M = Pd (**1a**), Pt (**1b**)] and $[Pd(\eta^3\text{-}2\text{-}Me\text{-}C_3H_4)]^+$ (**c**) building blocks in dichloromethane at room temperature, yielding the targeted homo-, that is, $[\{Pd(\eta^3\text{-}2\text{-}Me\text{-}C_3H_4)(PPh_2C_6F_4Py)_2\}_2\{Pd(dppp)\}_2](CF_3SO_3)_6$ (**1aL²c**), and heterotetrametallic, that is, $[\{Pd(\eta^3\text{-}2\text{-}Me\text{-}C_3H_4)(PPh_2C_6F_4Py)_2\}_2\{Pt(dppp)\}_2](CF_3SO_3)_6$, (**1bL²c**) metallamacrocycles in good yields (Scheme 3, left).

The NMR spectra of the larger macrocyclic species **L²** display a more complex solution dynamics than found for its **L¹** analogues described above. The resonances in the $^{31}P\{^1H\}$ NMR spectra assigned to the ligand **L²** (Figures S5 and S6 in the Supporting Information), for both **1aL²c** and **1bL²c**, are broad and indicative of an exchange process in solution involving the macrocyclic ring. Moreover, the dppp signal appears as a sharp singlet, which is in accordance with it being tightly bonded to the Pd or the Pt centres on the NMR time scale. The ^1H NMR spectra were found to be solvent and temperature dependent. Although the pattern in acetone solution is similar to that observed for the **L¹**-derived metallamacrocycles (Figures S7 and S8 in the Supporting Information), in $CDCl_3$ solution at 298 K only broad and poorly defined signals for all the coordinated ligands were obtained, which is in agreement with a very complex molecular movement in solution. Unfortunately, in this case, VT-^1H NMR spectroscopy in $CDCl_3$ did not provide further structural details about the dynamics of the system. Poorly defined spectra were obtained at temperatures in the 223–313 K range, and no trends could be inferred from the splitting of the very broad signals. Moreover, the fact that the fluorinated derivatives **1aL²c** and **1bL²c** showed only a moderate solubility in $CDCl_3$, hampered the study even more.

Fortunately, ESI-FTICR mass spectrometry strongly supports the formation of **1aL²c** and **1bL²c**. The mass spectra of these compounds show very informative peaks arising from the subsequent loss of anions from the parent metallamacrocycles (Figures 2 and S9 in the Supporting Information). As usually observed,[14] the more stable platinum derivative **1bL²c** undergoes lesser fragmentation and doubly $[\mathbf{1bL^2c}\text{-}2(CF_3SO_3)]^{2+}$, triply $[\mathbf{1bL^2c}\text{-}3(CF_3SO_3)]^{3+}$ and quadruply $[\mathbf{1bL^2c}\text{-}4(CF_3SO_3)]^{4+}$ charged species can be found in the mass spectrum (Figure 2).

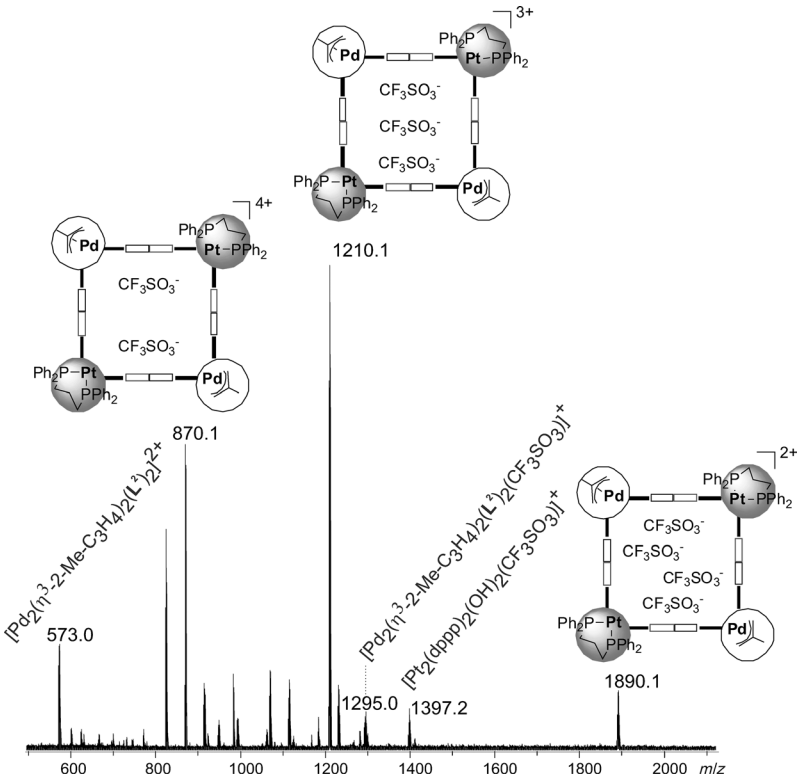

Figure 2. ESI-FTICR mass spectrum of **1bL²c** in acetone.

NMR evidences of metallacycle building block exchange

As reported in our previous communication,[5] the ^1H NMR spectra of both **1aL¹c** and **1bL¹c** in $CDCl_3$ at room temperature revealed two sets of signals for each α and β proton pairs of the pyridine rings, as well as four different peaks for the aliphatic protons of dppp (Figure S10 in the Supporting Information). When the ^1H NMR spectra were recorded at higher temperatures or in more coordinating solvents such as $[D_3]$nitromethane or $[D_6]$acetone, a trend to a simpler NMR pattern was observed. These changes imply a reversible cleavage of M–**L¹** bonds either at the phosphane corner {(dppp)M–N_{py}} (M = Pd, Pt) or at the allyl fragment {$(\eta^3\text{-}2\text{-}Me\text{-}C_3H_4)$Pd–P} (Scheme 3, right and bottom). These dissociation processes open up the possibility of envisaging an exchange between the supramolecular species and their constituent building blocks as a plausible alternative to a mere simple rotation

around the M–N_{py} bond that does not account for the observed NMR changes. With the aim of investigating these exchanges, we undertook a series of ^{1}H–^{1}H NOESY NMR experiments where the metallamacrocycles **1aL^{1}c** and **1bL^{1}c** were mixed in the NMR tubes with the appropriate stoichiometric amount of one of their building blocks. A NOESY experiment not only provides cross peaks due to NOE contacts but also cross peaks between mutually exchanging positions and consequently is a powerful technique for the investigation of chemical exchange in multisite systems.

In spite of the dynamical exchange, a 1:2 mixture of metallamacrocycle **1aL^{1}c** and the free corner **L^{1}c** in $CDCl_3$ showed separate α pyridine proton signals that displayed cross peaks in the ^{1}H–^{1}H NOESY NMR spectrum (Figure 3a). It is thus clear that there is a moderately fast exchange between the whole assembly [{Pd(η^3-2-Me-C_3H_4)(4-PPh_2py)$_2$}$_2${Pd(dppp)}$_2$](CF_3SO_3)$_6$ (**1aL^{1}c**) and its corresponding piece [Pd(η^3-2-Me-C_3H_4)(4-PPh_2py)$_2$](CF_3SO_3) (**L^{1}c**). Contrarily, the ^{1}H–^{1}H NOESY NMR spectrum of a mixture of the platinum analogue **1bL^{1}c** and the same **L^{1}c** block did not show evidence of ligand exchange because cross peaks between the α pyridine proton signals of **1aL^{1}c** and **L^{1}c** were not observed (Figure 3b) even at longer mixing times (1000 ms) and at the highest recommended temperature for $CDCl_3$ (313 K). These observations are in line with the higher inertness of the Pt–N_{py} bond when compared with the Pd–N_{py} bond.[14c]

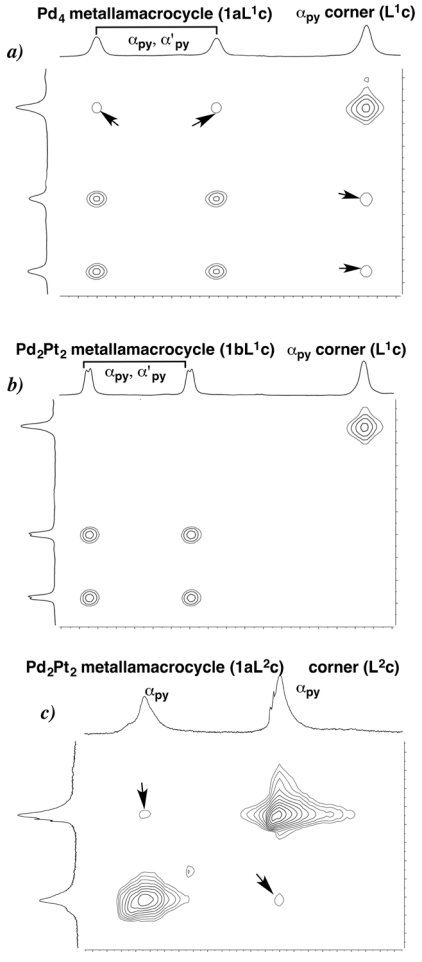

Figure 3. Section of the ^{1}H–^{1}H NOESY NMR spectra of a) a 1:2 mixture of metallamacrocycle **1aL^{1}c** and the free corner **L^{1}c** in $CDCl_3$ at 298 K (mixing time 500 ms), relevant cross peaks are indicated by arrows, b) a 1:2 mixture of metallamacrocycle **1bL^{1}c** and the free corner **L^{1}c** in $CDCl_3$ at 298 K (mixing time 1000 ms) and c) a 1:2 mixture of metallamacrocycle **1bL^{2}c** and the free corner **L^{2}c** in $CDCl_3$ at 298 K (mixing time 500 ms), relevant exchange cross peaks are indicated by arrows.

Interestingly, for the fluorinated metallacycle **1bL^{2}c**, exchange NOESY cross peaks (Figure 3c) are even observed when the Pt-containing heterometallic assembly is mixed with the appropriate corner **L^{2}c** in $CDCl_3$ at room temperature and at low mixing time (500 ms). The establishment of a dynamic equilibrium between the metallamacrocycles and their building blocks is thus further supported, as well as an exchange rate enhancement observed for the architectures derived from the fluorinated linkers. The worse donor character of the linker **L^2** induces a higher acidity of the Pt^{II} centre, and thus enables a faster associatively activated classical substitution process in **1bL^{2}c**.

The collected data do not rule out an alternative dynamic process involving the reversible dissociation of the Pd–P bond at the allylic **L^{n}c** corners.[15] In fact, the ^{1}H NMR spectrum of a 1:2 mixture of the **L^{1}c** palladium corner [Pd(η^3-2-Me-C_3H_4)(4-PPh_2py)$_2$](CF_3SO_3) and free 4-PPh_2py (**L^1**) in $CDCl_3$ shows a single broad signal assigned to the pyridine α protons, implying a very fast Pd–P dissociation equilibrium. Consequently, ^{1}H–^{1}H NOESY NMR experiments were conducted to study the exchange between **1aL^{1}c** and **1bL^{1}c** assemblies and the building block [M(dppp)(4-PPh_2py)$_2$]$^{2+}$ [M = Pd (**1aL^1**), M = Pt (**1bL^1**)] whose synthesis and characterisation is described in the Experimental Section. In spite of the fast equilibrium observed between the free 4-PPh_2py (**L^1**) and its palladium complex **L^{1}c**, no exchange cross peaks between the proton pyridine signals were observed between the **1aL^{1}c** and **1bL^{1}c** derivatives and the **1aL^1** and **1bL^1** blocks, respectively. These data confirm that the reversible dissociation of the M–N_{py} bond is the main process involved in the dynamic behaviour specifically observed in the reported metallamacrocycles.

In order to complement the exchange experiments indicated above, CH_2Cl_2 solutions containing the palladium metallamacrocycles **1aL^{1}c** or **1aL^{2}c** and the platinum corner **1b** in a 1:2 molar ratio were analysed by ^{31}P{^{1}H} NMR spectroscopy. In both cases, the ^{31}P{^{1}H} NMR spectra recorded immediately after mixing the components, show a complete exchange of the palladium fragment {Pd(dppp)} by the platinum fragment {Pt(dppp)} within the supramolecules (Scheme 4). Only the characteristic signals of the heterometallacycles **1bL^{1}c** or **1bL^{2}c**, as well as those of the free palladium corner **1a**, were found. The experiments confirmed not only the easy dissociation of the Pd–N_{py} bonds, but also the remarkable thermodynamic stability of the Pt–N_{py} bonds in the metallamacrocycle, responsible for the observed preference for these heterometallic assemblies (see below).

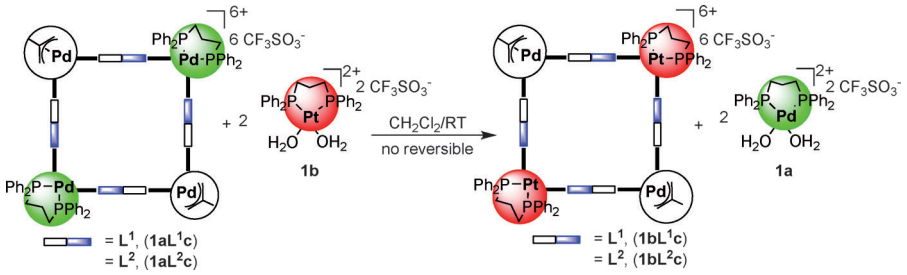

Scheme 4. Representation of the results obtained by using $^{31}P\{^1H\}$ NMR spectroscopy to clarify the exchange behaviour of the platinum and palladium supramolecules.

Electrospray ionisation mass spectrometry studies of the exchange between the metallamacrocycles

Electrospray mass spectrometry is a soft ionisation method that has been widely applied for the characterisation of supramolecules.[16] Because ESI-MS is able to identify the presence of multiple species simultaneously, it can be used to provide at least qualitative information on the composition of complex mixtures,[9d,17] and consequently it can be used to detect free components, reaction intermediates, wrongly assembled structures and the desired final thermodynamic assemblies that co-exist until equilibrium is reached. The technique is then very well suited for the characterisation of the dynamic block exchange processes as well as the subsequent thermodynamic equilibration that appear on the metallamacrocycles prepared. Thus, we carried out a series of ESI-MS experiments with the aim of determining the composition of the solutions obtained by mixing two different assemblies or their corresponding building blocks. All the experiments were undertaken in acetone to provide reliable and constant spray conditions in the electrospray ion source.

The ESI-MS analysis of an equimolar mixture of the metallacycles **1aL^{1}c** and **1bL^{1}c** reveals, together with the characteristic peaks of the individual compounds **1aL^{1}c** (m/z = 3159.1 [**1aL^{1}c**-$(CF_3SO_3)]^+$ and 1505.1 [**1aL^{1}c**-$2(CF_3SO_3)]^{2+}$) and **1bL^{1}c** (m/z = 3336.2 [**1bL^{1}c**-$(CF_3SO_3)]^+$ and 1593.1 [**1bL^{1}c**-$2(CF_3SO_3)]^{2+}$), further signals at m/z = 3248.1 and 1549.1 (Figure 4). Their isotopic distribution perfectly fits with the calculated pattern for these species resulting from the loss of one and two triflate anions from the nonsymmetrical **1a1bL^{1}c** mixed assembly, that is, $[\{Pd(\eta^3\text{-}2\text{-}Me\text{-}C_3H_4)(4\text{-}PPh_2py)_2\}_2\{Pd(dppp)\}\{Pt(dppp)\}](CF_3SO_3)_6$.

As shown in Figure 4, the ESI-MS spectrum obtained after 30 minutes of mixing shows a decrease of the intensity of the signals on increasing the number of palladium atoms in the assembly that is, the most intense peak corresponds to Pd_2Pt_2 (**1bL^{1}c**), whereas the least intense peak is assigned to Pd_4 (**1aL^{1}c**). Because the stoichiometry needs equimolar quantities of both precursors **1aL^{1}c** and **1bL^{1}c** in equilibrium with the mixed **1a1bL^{1}c** macrocycle, the observed intensity trend might be due, at least partially, to differences in the tendency toward fragmentation. These differences could be a consequence of the different kinetic and/or thermodynamic stability of the various species. Thus, the intermediate intensity of the mixed **1a1bL^{1}c** macrocycle clearly indicates that the existence of Pt–N_{py} bonds has a significant stabilising effect on these supramolecules. Moreover, the mass spectrum displays some additional peaks that correspond to aggregation species arising from the interaction of two different metallamacrocycles (**1aL^{1}c**/**1a1bL^{1}c**, **1aL^{1}c**/**1bL^{1}c** and **1bL^{1}c**/**1a1bL^{1}c**) with the loss of two triflate counter anions (Figure 4).

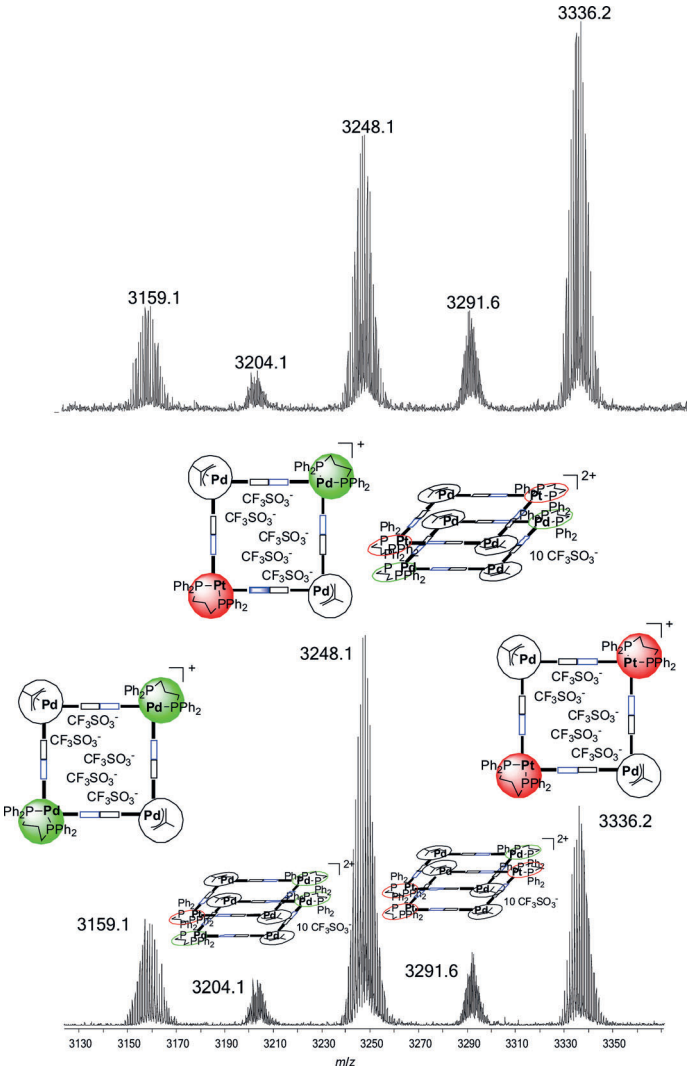

Figure 4. Section of the ESI-MS spectrum of a 1:1 mixture of **1aL^{1}c** and **1bL^{1}c** in acetone. Top) Taken after 30 minutes after mixing. Bottom) After the mixture has reached equilibrium.

It is interesting to note that, despite the fact that Pt–N_{py} bond dissociation has been found to be slower than the dissociation of the equivalent Pd–N_{py} bond (see above), the effective Pt–N_{py} bond dissociation has to take place to explain the formation of the species **1a1bL^{1}c** from the mixture of the two symmetric macrocycles **1aL^{1}c** and **1bL^{1}c**. Obviously, because of the relatively slow de-coordination of the Pt–N_{py} bonds, the formation of mixed **1a1bL^{1}c** takes place most probably without a full dissociation of the supramolecular assembly into mononuclear blocks. Nevertheless, the process demands the complete de-coordination of a {Pt(dppp)} corner and long times are required for equilibration (Figure 4, bottom). The final speciation in solution thermodynamically compensates the loss of two Pt–N_{py} bonds in **1bL^{1}c** by the change of two Pd–N_{py} bonds in **1aL^{1}c** to two new Pt–N_{py} bonds in **1a1bL^{1}c** (Scheme 5, bottom).

To prove that the mixed Pd_3Pt metallamacrocycle (**1a1bL^{1}c**) was not a species that results from the assembly of different fragments in the ESI source, the ESI-MS spectrum of an acetone solution of the symmetrical compound **1bL^{1}c** with the palladium corner $[Pd(H_2O)_2(dppp)](CF_3SO_3)_2$ (**1a**) in a 1:2 molar ratio was recorded. Only the peaks corresponding to the starting materials were observed, thus indicating that no exchange between the Pt and Pd corners in the metallamacrocycles takes place in the mass spectrometer. Furthermore, the experiment proves the enhanced thermodynamic stability of the Pt–N_{py} bonds, whose de-coordination cannot be energetically compensated in this case.

The respective ESI mass studies on the composition of mixtures obtained from the fluorinated **L^2** derivatives, that is, **1aL^{2}c** and **1bL^{2}c**, produced equivalent results. The formation of the mixed assembly **1a1bL^{2}c** was confirmed by a signal at $m/z = 1845.1$, assigned to the doubly charged $[\mathbf{1a1bL^2c}\text{-}2(CF_3SO_3)]^{2+}$, arising from the loss of two triflate anions from the mixed macrocyclic assembly (Figure S11 in the Supporting Information).

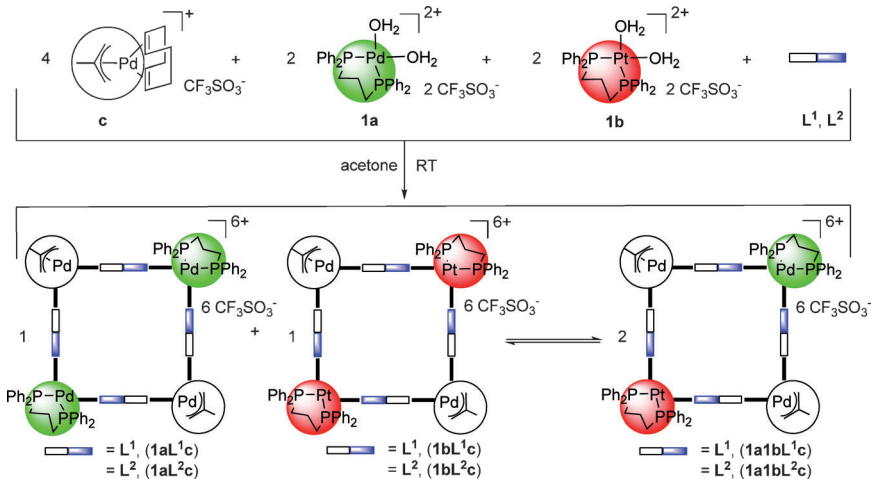

Scheme 5. Reaction scheme for the formation of the mixed **1a1bL^{1}c** and **1a1bL^{2}c** mixed species.

NMR evidence for the exchange between metallamacrocycles

In addition to the mass spectrometric characterisation indicated above, supportive time-dependent NMR studies were employed to characterise the exchange processes between the metallamacrocycles. To this end, a $^{31}P\{^1H\}$ NMR spectrum was recorded immediately after mixing in [D$_6$]acetone equimolar quantities of **1aL^{1}c** and **1bL^{1}c**. The spectrum showed in addition to the signals of the two equivalent phosphorus atoms of the 4-PPh_2py ligands attached to the $\{Pd(\eta^3\text{-}2\text{-}Me\text{-}C_3H_4)\}^+$ unit in either **1aL^{1}c** or **1bL^{1}c**, a coupled ($^2J(P,P)_{simulated} = 34$ Hz) pair of doublets (centred at $\delta_{simulated} = 24.4$ and 24.9 ppm, respectively) partially overlapped with the former signals. The observed second-order NMR pattern (Figure 5) agrees well with the lower symmetry expected for the Pd_3Pt metallacycle **1a1bL^{1}c**, where the phosphorus signals of the ligand **L^1** in the asymmetric assembly **1a1bL^{1}c** are not chemically equivalent. As expected from the ESI data (Figure 4), the intensity of these doublets increases with time, reaching equilibrium after approximately 48 h (Figure 5).

The equilibrated molar ratio **1aL^{1}c**:**1bL^{1}c**:**1a1bL^{1}c** is roughly 1:1:2, which corresponds to a minimum of energy of the system. Time-dependent ^{1}H NMR spectra showed exactly the same behaviour. After 48 h three very close ($\Delta\delta < 0.01$ ppm) singlets centred at $\delta = 1.96$ ppm were observed, that were assigned to the methyl signals of the allyl moiety for **1aL^{1}c**, **1a1bL^{1}c** and **1bL^{1}c**, respectively. The other proton signals are not affected by the loss of symmetry on going from **1aL^{1}c** and **1bL^{1}c** to **1a1bL^{1}c** and appear superimposed with that of the symmetrical **1aL^{1}c** and **1bL^{1}c** metallamacrocycles. NMR spectra corre-

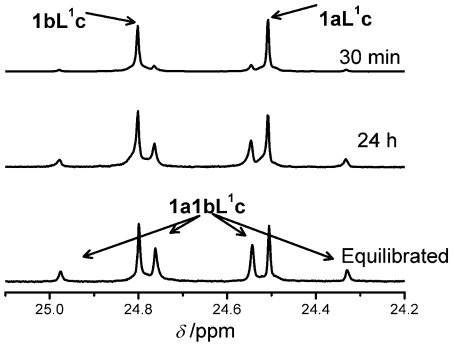

Figure 5. Time-dependent $^{31}P\{^1H\}$ NMR spectra of a 1:1 mixture of **1aL^{1}c** and **1bL^{1}c** in [D$_6$]acetone. The represented region corresponds to the PPh_2 signals of the ligand **L^1** in the indicated metallamacrocyclic compounds.

sponding to the final equilibrium speciation were also obtained immediately after mixing **1a**, **1b**, **c** and **L**^{n} (or **L**^{n}**c**) building blocks in the appropriate molar ratio, indicating that the attainment of the equilibrium in this case does not require the dissociation of already formed Pt–N_{py} bonds and the most thermodynamically favourable composition is immediately reached (Scheme 5). Once the NMR spectra indicated that the equilibrium was reached, the solutions were analysed by ESI mass spectrometry and, although this system does not allow ESI-MS quantification as indicated above, a clear predominance of the mixed metallamacrocycle **1a1bL^{1}c** was observed (Figure 4, bottom).

The NMR study of mixtures obtained from the fluorinated **L^{2}** derivatives did not prove to be definitive about the formation of mixed Pd_3Pt **1a1bL^{2}c** metallamacrocycles. In addition to the expected singlets assigned to dppp in the metallacycles, the $^{31}P\{^{1}H\}$ NMR spectra showed a broad signal at $\delta = 9.3$ ppm that can be assigned to the overlapping of the four different **L^{2}** phosphorus resonances arising from **1aL^{2}c**, **1bL^{2}c** and **1a1bL^{2}c** in fast exchange (Figure S12 in the Supporting Information), agreeing with the enhanced lability found for the **L^{2}** systems. It is interesting to note that, in this case, the mass spectra did not show dependence with time, which indicates that the equilibrium is reached immediately after mixing, which is in accordance with the enhanced mobility observed for the fluorinated **L^{2}** system.

served in the ^{1}H NMR spectra has been conducted for compounds **1aL^{1}c**, **1bL^{1}c**, **2aL^{1}c** and **2bL^{1}c** in different solvents and with different amounts of added triflate anions. The solvent and the triflate concentration have been screened to address if mild coordination media can be involved in the substitution processes indicated before. Similar studies of these effects on systems with much better donor anions have already been reported.[9b,c] Table 1 collects the relevant kinetic and thermal activation parameters for the systems studied in solution at different temperatures, and Figure 6 shows a typical rate simulation by using the gNMR software[19] as well as their corresponding Eyring plots for the determination of $\Delta H^{\neq}$ and $\Delta S^{\neq}$. The analogous fluorinated compounds **1aL^{2}c** and **1bL^{2}c** have not been studied, being always in the fast exchange regime regardless of the temperature and/or the solvent used.

Table 1. Kinetic and thermal activation parameters determined for the dynamic behaviour observed for the metallamacrocyclic systems studied (Schemes 1 and 3) in different solution media and 2×10^{-3} M macrocycle concentration.

Compound	Solution medium	^{273}k [s^{-1}]	$\Delta H^{\neq}$ [kJ mol^{-1}]	$\Delta S^{\neq}$ [J K^{-1} mol^{-1}]
1aL^{1}c	$CDCl_3$	7.3[a]	(46±3)[a]	(−61±10)[a]
	$CDCl_3$ + 10-fold $(NBu_4)CF_3SO_3$ added	20[a]	(26±1)[a]	(−126±4)[a]
	CD_3NO_2	7.6	(59±2)	(−13±7)
1bL^{1}c	$CDCl_3$	1.4	(53±5)	(−49±16)
	$CDCl_3$ + 10-fold $(NBu_4)CF_3SO_3$ added	1.4	(49±4	(−64±16)
	CD_3NO_2	2.8	(58±4)	(−25±13)
2aL^{1}c	$CDCl_3$	600	(19±3)	(−123±10)
	$CDCl_3$ + 10-fold $(NBu_4)CF_3SO_3$ added	700	(41±2)	(−41±7)
	CD_3NO_2	420	(21±2)	(−126±7)
2bL^{1}c	$CDCl_3$	70	(22±2)	(−130±8)
	$CDCl_3$ + 10-fold $(NBu_4)CF_3SO_3$ added	60	(33±3)	(−91±9)
	CD_3NO_2	55	(28±2)	(−110±9)

[a] Taken from reference [5].

Kinetic studies on the exchange dynamics

As indicated in the previous sections, the gross dynamics in solution of the prepared metallamacrocycles is reflected by the ^{1}H NMR signal behaviour of the α,α′ and β,β′ pyridine protons of the **L^{1}** and **L^{2}** linkers. According to the X-ray structure of **1bL^{1}c**,[5] the four pyridine protons of these linkers should be non-equivalent, each α and β proton being in a different relative position with respect to the methyl group of the allyl ligand of the **c** unit (Figure 1).[5] These signals are usually rather broad, when observed separately, and even coalesce to a single set in several cases. This dynamic behaviour has already been observed in a wealth of situations, and involves the macroscopic movement of the linkers on the metal centres in solution.[17e,18] Although rotation of the M–N_{py} bond can account for the dynamic behaviour on the NMR time scale,[9b,c,10] this is not the case in the present situation and exchange processes have been observed (see the previous sections) between assembled and free building blocks.

In view of the results obtained in the preliminary studies carried out on **1aL^{1}c**, the kinetic monitoring of the dynamics ob-

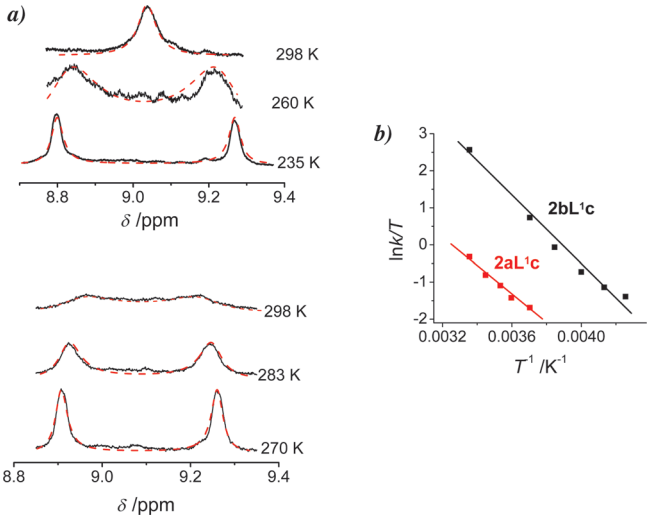

Figure 6. a) Line-shape analysis (red dashed line) of the resonances of the ^{1}H NMR spectra ($CDCl_3$, 500 MHz) of the α and α′ proton pairs in compounds **2aL^{1}c** (top) and **2bL^{1}c** (bottom). b) Eyring plots for the kinetic exchange parameters for the same compounds.

The data in Table 1 correspond to the gross reversible dissociation of **1a**, **1b**, **2a** and **2b** fragments from $\mathbf{L^1c}$ blocks, as established from the ESI-MS and VT-NMR experiments indicated above and in our preliminary communication.[5] The process necessarily has to involve the coordination of another Lewis base present in the medium such as the solvent, the six triflate anions already present in the species, or those specifically added (10-fold, i.e., 60 anions per macrocycle). From the data it is clear that at 273 K the overall exchange process measured is faster for the palladium derivatives (5–10-fold); nevertheless, the difference in the values does not agree with the expected much larger lability of the Pd–N bond (10^5–10^6-fold) with respect to the Pt–N analogue.[12b] Given the fact that the data correspond to an effective intermolecular exchange of the M–N_{py} bonds, it is clear that the already reported cooperative labilisation in large self-assembled structures is of key importance in the observed solution behaviour.[17e,20] As for the thermal activation parameters obtained, all of them indicate a clear associativeness of the process, especially for the PPh_3 systems ($\mathbf{2aL^1c}$ and $\mathbf{2bL^1c}$), were the activation entropies are more negative, whereas $\Delta H^{\neq}$ has lower values. Probably, the much more flexible environment around the metal centres in **2a** and **2b**, as well as the worse donor character of the ligand, enable a better transient association of an incoming ligand in the coordination sphere of the metal.[12b] This seems, in fact, to be the determinant factor that differentiates dppp from PPh_3 macrocyclic systems. In this respect, the fact that the $\mathbf{L^2}$ analogues show a much faster dynamic exchange can also be associated to the worse donor character of the fluorinated ligand.

The values obtained for the same systems in nitromethane solution, also collected in Table 1, do not show any significant trend with respect to the data in chloroform, thus indicating the relative innocence of both solvents in the process, despite the small differences observed in the ^{1}H NMR experiments. In this respect, the fact that the ^{1}H NMR spectra in [D_6]acetone at room temperature already show the coalescence of the pyridine proton pairs is indicative of the much better donor character of this solvent (Gutmann's DN^N being 0.0 kcal mol^{-1} for chloroform, 2.7 kcal mol^{-1} for nitromethane and 17 kcal mol^{-1} for acetone).[21]

With respect to the data obtained from the experiments carried out in chloroform solution containing a 10-fold excess of tetrabutylammonium triflate (60:1 triflate/macrocycle ratio), they merit a special consideration. Any difference has to involve a dominant interaction with the large amount of weakly coordinating triflate anions present in the reaction medium. Although for the platinum-containing systems $\mathbf{1bL^1c}$ and $\mathbf{2bL^1c}$ no relevant changes are observed, for the palladium species $\mathbf{1aL^1c}$ and $\mathbf{2aL^1c}$ important differences are evident between their thermal activation parameters at 10-fold excess of tetrabutylammonium triflate (60:1 triflate/macrocycle ratio) and those obtained under stoichiometric conditions (6:1 triflate/macrocycle ratio) ($\approx$20 kJ mol^{-1} for $\Delta H^{\neq}$ and 70 J K^{-1} mol^{-1} for $\Delta S^{\neq}$, see Table 1). Clearly, the more labile and polarising character of the smaller palladium units in the macrocycle have to be responsible for the difference between the observed behaviour of the platinum and palladium macrocycles. One should take into account that ion pairing is an omnipresent feature in these systems and its formation has already been held responsible of simple first order kinetics for nitrate substitution-activated exchange processes,[9d] as well as in molecular recognition. In fact, there are examples where molecular recognition has been found to be more important for palladium- than for analogous platinum-containing architectures.[14d] Interestingly, although the results for the dppp $\mathbf{1aL^1c}$ macrocycle indicate that the gross exchange process increases its associative character (smaller $\Delta H^{\neq}$ and more negative $\Delta S^{\neq}$ values) on increasing the concentration of triflate anions in the reaction medium, the opposite is observed for the PPh_3 $\mathbf{2aL^1c}$ analogue.

From the data shown in the previous sections, the only way to come to terms with this difference demands that, depending on the metallamacrocycle, the rate-dominant process for the exchange corresponds to different reactions. For $\mathbf{1aL^1c}$ (the macrocycle with a more acidic and less hindered Pd centre) the dominant reaction, on increasing the quantities of triflate anions present, moves from the pyridine by triflate substitution on the initial $\mathbf{1aL^1}$ units (more dissociative) to the back coordination of a $\mathbf{L^1c}$ ligand to the de-coordinated {(dppp)Pd-triflate} fragments (more associative). This shift is not surprising in the presence of large amounts of tributylammonium triflate. For the macrocycle $\mathbf{2aL^1c}$ (with the less acidic and more hindered Pd centre), large amounts of {$(PPh_3)_2$Pd-triflate} fragments are expected even at low triflate concentrations, thus providing a more associative character of the substitution even under these conditions. As a result, the dominant operation of the more dissociative substitution process on the {$(PPh_3)_2$Pd-N_{py}} units at high triflate concentrations has to be related with the sequestering of the above-mentioned {$(PPh_3)_2$Pd-triflate} fragments by formation of dead-end outer-sphere complexes by association to the increasing amounts of triflate anions.[22]

Preliminary catalytic studies

Allyl Pd^{II} complexes stabilised with phosphine ligands are good catalytic precursors for the catalysed allylic alkylation reaction.[6] The activity and selectivity of the process depends on several factors such as the structure of the allyl substrate, the ligand or nucleophile and the nature of the solvent.[7] The regioselectivity of the allylic alkylation of a monosubstituted allylic substrate depends on the nature of the ligand used. When a symmetrical diphosphine is used the substitution occurs mainly at the terminal carbon atom leading to the linear substituted product[23] but the use of sterically bulk monophosphines or unsymmetrical ligands reverse the regiochemistry to the branched product.[23a,24] The metallamacrocycles described in this paper represent promising accessible palladium allyl complexes with monodentate ligands, whereas having properties associated to bidentate chelating systems. In this respect, interesting reports dealing with the effect on catalytic processes of metal complexes containing self-assembled supramolecular bidentate ligands exist in the literature.[25]

In this line we have studied the effect on both the activity and the regioselectivity of the allylic alkylation of the *rac*-3-ace-

toxy-1-phenyl-1-propene catalysed by the macrocycles **1aL^{1}c** and **1bL^{1}c**. The reaction was performed by using the sodium salt of dimethylmalonate as the nucleophile in CH_2Cl_2 at room temperature and with 0.5 mol% of concentration level of catalyst (Scheme 6). A blank study by using 1 mol% of the mononuclear palladium corner **L^{1}c** has also been conducted for comparative purposes; the results obtained are collected in Table 2.

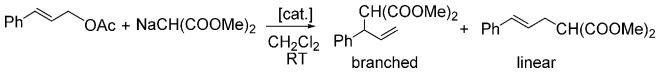

Scheme 6. Reaction scheme of the studied catalytic reaction.

Table 2. Catalytic results of the allylic alkylation of *rac*-3-acetoxy-1-phenyl-1-propene according to Scheme 6.[a]

Precursor	Conversion [%]	Branched/linear
L^{1}c[b]	100	12:88
1aL1c[c]	95	13:87
1bL1c[c]	50	14:86

[a] Catalytic conditions: 1 mmol *rac*-3-acetoxy-1-phenyl-1-propene, 3 mmol $NaCH(COOMe)_2$, 8 mL CH_2Cl_2 at RT for 1 h. Conversion and branched:linear ratio determined by GC. [b] 1×10^{-2} mmol catalytic precursor. [c] 0.5×10^{-2} mmol catalytic precursor.

The total conversion and a 12:88 branched/linear ratio of the alkylation product was obtained after one hour reaction when the mononuclear **L^{1}c** corner was used as catalytic precursor. Similar results, both in activity and regioselectivity, have been reported[23a] for the analogous compound $[Pd(\eta^3\text{-}C_3H_5)(PPh_3)_2]^+$ prepared in situ: 99% conversion with a 9:91 ratio at $-20\,^\circ C$ after twelve hours of reaction in thf with $NaCMe(COOMe)_2$ as nucleophile. Clearly, the presence of a distant nitrogen donor in the phosphine ligands does not have any relevant effect on either the regioselectivity or the activity of the alkylation process. On moving to the metallamacrocycles described in this work, some differences are observed between the compounds **1aL^{1}c** and **1bL^{1}c**. Whereas the palladium metallamacrocycle **1aL^{1}c** shows a similar activity to that of the corner species **L^{1}c**, the heterometallic palladium–platinum assembly, **1bL^{1}c**, displays a lower activity, which parallels the observed lower exchange rate of the allylic corner **L^{1}c** with the metallamacrocycle **1bL^{1}c**, with respect to the same process on **1aL^{1}c**. It seems clear that the fragment **L^{1}c** in the metallacycle is less prone to a nucleophilic attack or/and an oxidative addition of the substrate than in the unassembled form. Nevertheless, complete conversion is achieved after six hours of reaction with both macrocycles. As indicated in Table 2, the same regioselectivity was obtained for the mononuclear **L^{1}c** and both metallamacrocycles **1aL^{1}c** and **1bL^{1}c**. In our macrocyclic systems the more rigid environment of the allyl palladium fragment $\{Pd(\eta^3\text{-}2\text{-}Me\text{-}C_3H_4)\}$ when assembled into the metallamacrocycle does not have any effect on the regioselectivity of the catalytic process. The same sort of behaviour has already been described by Hayashi et al.[23a] when the bidentate ligand dppe was used instead of the monodentate PPh_3 (89:11 ratio linear/branched regioisomers).

Discussion

In view of the results collected so far, it is clear that all the metallamacrocyclic assemblies prepared in this work are labile, unlike other compounds found in the literature,[17e,26] despite showing a high thermodynamic stability. Although for the Pd_4 compounds, that is, **1aL^{1}c**, **2aL^{1}c** and **1aL^{2}c**, this is somehow expected, for the Pd_2Pt_2 derivatives, that is, **1bL^{1}c**, **2bL^{1}c** and **1bL^{2}c**, a rather unusual intrinsic labilisation is observed, which is reflected in the dynamic behaviour of different fragments at room temperature. Taking into account that not even a salt-mediated substitution acceleration is observed,[27] and that the expected changeover from associative to dissociative activation for substitution reactions on Pt^{II} organometallic complexes is not relevant in these complexes,[28] this is an extremely remarkable feature. A similar effect has already been observed in compounds containing good π-acceptor pyridine derivative ligands.[29] The presence of two phosphane donors in the coordination sphere of the Pt^{II} centres probably creates a similar reinforced *trans* effect on the attached linkers **L^1** and **L^2**, thus enabling its increased labile substitution behaviour.

However, even with fairly uniform gross dynamic behaviour of the pyridine α protons, the results reported indicate the existence of differences between the assembly/disassembly dynamics of the palladium and platinum metallamacrocyclic systems. Whereas NOESY NMR experiments conducted with the palladium species **1aL^{1}c** indicate that the macrocyclic unit is in effective exchange, at the magnetisation transfer time scale, with free corner **L^{1}c** added to the reaction medium, this is not so for the platinum species **1bL^{1}c**. These differences necessitate of a rather complex behaviour of the metallamacrocycles in solution. The overall dynamics should distinguish between the movement making the α pyridine protons of ligand **L^1** equivalent from that leading to the exchange of the **L^{1}c** fragment. These processes are collected as an example in Scheme 7 for the **L^1** dppp derivatives; the first reaction at the left side corresponds to the one related to the α pyridine protons exchange (Figure 1), whereas the one at the centre corresponds to the exchange of the **L^{1}c** and/or **1a** or **1b** fragments (Figure 3).

For the all-palladium macrocycles both processes are within the NMR time scale, whereas for the platinum compound **1bL^{1}c** the exchange with the **L^{1}c** fragment is not observed on this time scale. Contrarily, for the closely related platinum derivative **1bL^{2}c** the magnetisation-transfer process with the **L^{2}c** corner is observed, agreeing with an easier substitution process on the **1bL^2** fragment containing the poorer donor, that is, the fluorinated ligand **L^2**. Within the same context, the palladium fragments **1a** were found to exchange faster than the equivalent platinum units **1b**, which indicated the greater lability of the former within the metallamacrocycle, which leads to the thermodynamic preference of the Pt-containing molecules.

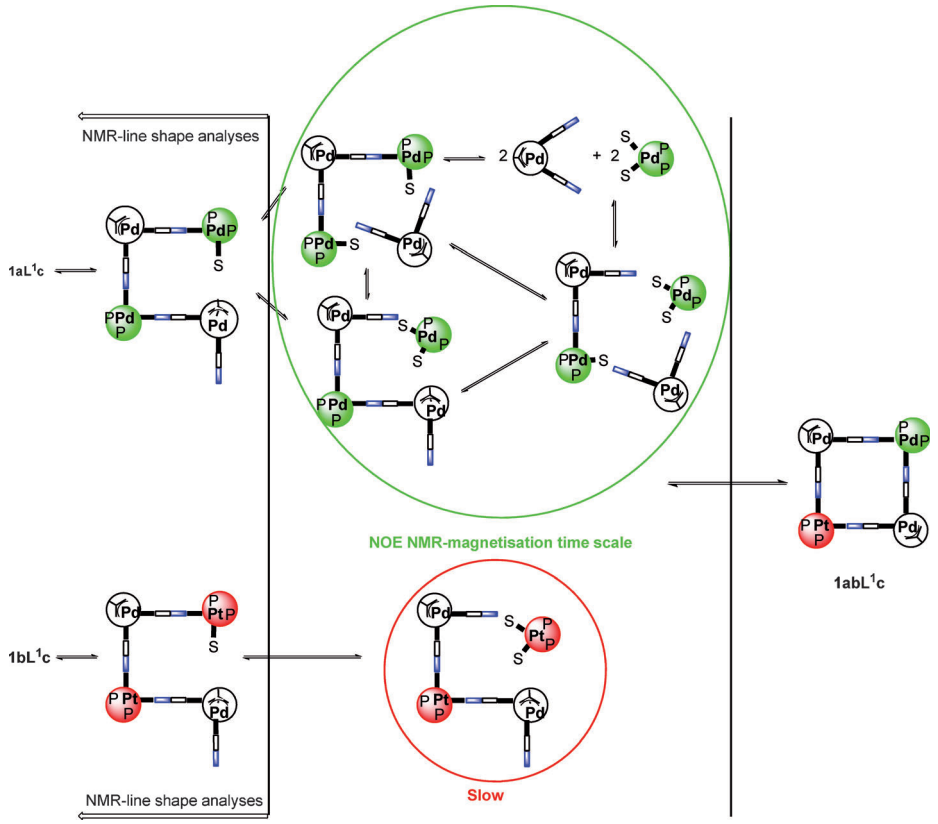

Scheme 7.

Summarising, in Scheme 7 labilisation of the Pt–N_{py} bond to a level similar to the Pd–N_{py} analogue is indicated on the macrocyclic units. The dynamic process thus observed for the α,α' pyridine protons corresponds to the formation of an open form on the cycle, which enables a free rotation of the structures making them equivalent. Once the macrocycle has been opened by the dissociation of one of the M–N_{py} bond, the lability of the M–N_{py} bonds is reduced considerably and no exchange evidences can be inferred from line shape analysis NMR experiments. In a moderately fast time scale, for the dppp palladium (**1a**) and/or $\mathbf{L^2}$ systems, further dissociation of the M–N_{py} bonds can take place. The latter produces a magnetisation exchange with the respective free $\mathbf{L^1c}$ or $\mathbf{L^2c}$ fragments, and the effective exchange of the palladium blocks by the platinum analogues, producing thermodynamically stable mixed Pd/Pt derivatives, is observed (Scheme 7, right). The final outcome being the consequence of the ${}^{diss}k_{Pd-N_{py}}/{}^{diss}k_{Pt-N_{py}}$ rate constant ratio.

The ESI-MS experiments carried out fully agree with the data collected by magnetisation transfer and/or line shape analysis NMR experiments. The favourable formation of new more inert Pt–N_{py} bonds is observed from mixtures of the metallamacrocycles $\mathbf{1aL^1c}$ and $\mathbf{1bL^1c}$ producing mixed compounds $\mathbf{1a1bL^1c}$ in a relatively slow process originated by the total disassembly of a platinum unit **1b** from the open form of the macrocycle $\mathbf{1bL^1c}$ (Scheme 7, centre). NMR experiments have also indicated that the process is slow and needs approximately 48 hours to reach equilibrium. In this respect, for the experiments carried out on the much more labile systems $\mathbf{1aL^2c}$ and $\mathbf{1bL^2c}$, a shorter equilibration time is observed, which is in agreement with the more labile nature of the Pt–N_{py} bond of the units $\mathbf{1bL^2}$.

Interestingly, the triflate concentration effects seen in the reversible opening process (Scheme 7, left) can also be rationalised. Although for the opening of the platinum-containing metallamacrocycles only the dissociation of the initial Pt–N_{py} bond is relevant and no changes in the associativity are expected, for the palladium-containing macrocycles, an increase of the triflate concentration has to increase necessarily the amount of fully disassembled units **1a** or **2a**, thus producing the effects related to the increasing amounts of either {(dppp)Pd-triflate} or $\{(PPh_3)_2$Pd-triflate$\}$ fragments indicated before, that is, an increased associativity/discrimination character of the exchange process.

The results collected for the catalytic process studied also agree with the general dynamic speciation behaviour observed in ESI-MS, magnetisation-transfer NMR and time-dependent NMR experiments. Clearly, the opening and disassembling of the metallamacrocycles represent the keystone for the data collected in Table 2, where the results are compared with those obtained for the corner $\mathbf{L^1c}$ under the same conditions. When the Pd^{II} allyl fragment $\mathbf{L^1c}$ is tightly anchored to the macrocycle, the activity of the alkylation process decreases. As a consequence, the larger catalytic activity corresponds to compound $\mathbf{1aL^1c}$ where the formation of the open form of the macrocycle is faster and its disassembly to individual pieces more favoured.

Conclusion

The supramolecular metallamacrocycles $\mathbf{1aL^1c}$, $\mathbf{1bL^1c}$, $\mathbf{2aL^1c}$, $\mathbf{2bL^1c}$, $\mathbf{1aL^2c}$, $\mathbf{1bL^2c}$ and $\mathbf{1a1bL^1c}$ can be obtained through self-assembly reactions of different combinations of building blocks. The obtained metallamacrocycles are stereochemically non-rigid and their dynamic process depends on the solvent, the basicity of the ligands and/or the size of the metallamacrocycles. The kinetico-mechanistic studies conducted corroborate that the pyridine dissociation of the metal is needed to explain the line shape analysis of the NMR spectra. NOE magnetisation transfer experiments indicate that further dissociation into the

building blocks has to take place in order to explain the full comprehensive mechanistic assembly/disassembly processes.

The results confirm the slower kinetics of Pt–N_{py} versus Pd–N_{py} bond, despite its increased lability in the fully assembled metallamacrocycle. In all cases, the platinum-containing assemblies show an enhanced thermodynamic stability that accounts for the assembly of mixed asymmetric architectures on mixing symmetrical analogues.

The introduction of allyl-palladium moieties in metallamacrocycles did not improve the catalytic activity or regioselectivity of the corresponding active monometallic complex in the allylic substitution reaction. However, as a future prospect, we envisage the introduction of chiral building blocks near the catalytic centres in the supramolecular species in order to widen the scope of the strategy and induce stereoselectivity in the studied catalytic process.

Experimental Section

All manipulations were performed under pre-purified N_2 by using standard Schlenk techniques. Infrared spectra were recorded on an FT-IR 5700 Nicolet spectrophotometer. Solvents were dried by standard methods and distilled under argon or nitrogen immediately prior to use, or alternatively from a solvent purification system (Innovative Technologies). $^{31}P\{^1H\}$ NMR (δ(85% H_3PO_4) = 0.0 ppm), ^1H NMR (δ(TMS) = 0.0 ppm) and ^{19}F NMR ($\delta(CFCl_3) = 0.0$ ppm) spectra were obtained on a Bruker DXR 250, a Varian-Inova 300, a Varian Mercury 400, a Varian-Inova 500 or a Bruker DMX 500 spectrometer. ESI mass spectra were recorded on a Bruker APEX IV Fourier-transform ion cyclotron resonance mass spectrometer with a 7.05 T magnet and an Apollo electrospray (ESI) ion source equipped or on a LC/MSD-TOF (2006) (Agilent Technologies) (G1969A). Typically, acetone solutions of the metallacycles (0.1–0.2 mM) were used with flow rates of 3–4 or 10 $\mu L\,min^{-1}$ depending on the spectrometer used. Elemental analyses of C, H, N and S were carried out at the Institut de Bio-Orgànica in Barcelona. Line shape analyses of exchanging signals were performed by using the gNMR software package.[19] All the rate constants obtained for the different systems under various conditions are collected in Table S1 in the Supporting Information.

The compounds 4-PPh_2py,[30] 4-BrC_6F_4py,[11] [$M(H_2O)_2$(dppp)]-(CF_3SO_3)$_2$ (M = Pd, Pt),[31] [$MCl_2(PPh_3)_2$] (M = Pd, Pt),[32] [$Pd(H_2O)_2$-(PPh_3)$_2$](CF_3SO_3)$_2$,[33] [Pd(μ-Cl)(η^3-2-Me-C_3H_4)]$_2$,[34] [Pd(η^3-2-Me-C_3H_4)-(cod)](CF_3SO_3),[35] and [{Pd(η^3-2-Me-C_3H_4)(PPh_2py)$_2$}$_2${M(dppp)}$_2$]-(CF_3SO_3)$_6$ [M = Pd (**1aL^1**), Pt (**1bL^1**)],[5] were prepared as described previously. All other chemicals were commercial grade and were used without further purification.

General procedure for Pd-catalysed allylic alkylation of *rac*-3-acetoxy-1-phenyl-1-propene: Reactions were carried out in a Schlenk tube under N_2 at room temperature. The Pd^{II} precursor (0.01 mmol for the monomer complex **L^{1}c** and 0.005 mmol for metallamacrocycles **1aL^1** or **1bL^1**) was dissolved in CH_2Cl_2 (1 mL) and *rac*-3-acetoxy-1-phenyl-1-propene (1 mmol) in CH_2Cl_2 (1 mL) was added. After 15 min. stirring Na(CH(COOMe)$_2$) (3 mmol) in CH_2Cl_2 (6 mL) was added. The mixture was stirred at room temperature for the desired time (1 or 6 h). Then, the solution was diluted with diethyl ether (20 mL) and washed with saturated ammonium chloride solution (3×10 mL) and water (3×10 mL). The organic phase was dried over anhydrous Na_2SO_4 and filtered off, and the solvent was removed under reduced pressure. Conversion was determined by ^1H NMR spectroscopy. Purification of the product was done by column chromatography (SiO_2, ethyl acetate). Conversion and the regioisomeric ratio (linear/branched) were determined by GC on an Agilent HP-5 column.

Synthesis of 4-$PPh_2C_6F_4$py (L^2): An hexane solution of *n*BuLi (1.6 M, 1 mL) was added dropwise to a pre-cooled (−78 °C) solution of BrC_6F_4py (465 mg, 1.52 mmol) in thf (60 mL). After 1 h of stirring, the mixture was allowed to warm slowly to −40 °C. Then, the solution was cooled again to −78 °C and a solution of PPh_2Cl (0.29 mL, 1.52 mmol) in thf was added dropwise. The mixture was allowed to warm slowly to room temperature and concentrated to dryness to give a yellow oil that was treated with CH_2Cl_2. The obtained suspension was filtered and concentrated to dryness. Re-crystallisation from ethanol of the solid residue gave a white crystalline solid in 65% yield (406 mg). ^1H NMR (298 K, $CDCl_3$): δ = 8.76 (d, J(H,H) = 6.1 Hz, 2H; $H_{\alpha\text{-py}}$), 7.51–7.46 (m, 4H; Ph_{ortho}), 7.42–7.39 ppm (m, 8H; $H_{\beta\text{-py}}$, $Ph_{meta+para}$); $^{31}P\{^1H\}$ NMR (298 K, $CDCl_3$): δ = −24.6 ppm (t, ^3J(P,F) = 37 Hz); ^{19}F NMR (298 K, $CDCl_3$): δ = −127.6 (m, 2F; F_x), −142.4 ppm (m, 2F; F_A); IR (KBr): $\tilde{\nu}$ = 1458, 1430, 970 cm^{-1}; ESI(+) m/z: 412.1 $[M+H]^+$; calcd: 412.1; elemental analysis calcd (%) for $C_{23}H_{14}F_4NP$: C 67.16, H 3.43, N 3.40; found: C 66.98, H 3.41, N 3.43.

Synthesis of [Pd(η^3-2-Me-C_3H_4)(4-PPh_2py)$_2$](CF_3SO_3) (L^{1}c): Solid [Pd(η^3-2-Me-C_3H_4)(cod)](CF_3SO_3) (250 mg, 0.59 mmol) was added to a solution of 4-PPh_2py (314 mg, 1.19 mmol) in dichloromethane (40 mL) at room temperature. After 15 min of stirring, the reaction mixture was filtered, concentrated to 10 mL under vacuum and precipitated with diethyl ether. A pale grey solid was obtained in 75% yield (375 mg). ^1H NMR (298 K, $CDCl_3$): δ = 8.41 (d, J(H,H) = 2.4 Hz, 4H; $H_{\alpha\text{-py}}$), 7.52–7.37 (m, 20H; Ph), 6.99 (d, J(H,H) = 2.06 Hz, 4H; $H_{\beta\text{-py}}$), 4.06 (s, 2H; Me-C_3H_4), 3.72 (s, 2H; Me-C_3H_4), 1.85 ppm (s, 3H; *Me*-C_3H_4); ^1H NMR (298 K, [D_6]acetone): δ = 8.49 (d, J(H,H) = 2.4 Hz, 4H; $H_{\alpha\text{-py}}$), 7.62–7.47 (m, 20H; Ph), 7.12 (d, J(H,H) = 5.2 Hz, 4H; $H_{\beta\text{-py}}$), 3.99 (s, 2H; Me-C_3H_4), 3.83 (t, J(H,P) = 5.2 Hz, 2H; Me-C_3H_4), 2.06 ppm (s, 3H; *Me*-C_3H_4); $^{31}P\{^1H\}$ NMR (298 K, $CDCl_3$): δ = 21.7 ppm (s); IR (KBr): $\tilde{\nu}$ = 1615, 1480, 1438, 1262, 1150, 1110, 1031 cm^{-1}; ESI(+): m/z: 687.1 $[M-CF_3SO_3]^+$; calcd: 687.1; elemental analysis calcd (%) for $C_{39}H_{35}F_3N_2O_3P_2PdS$: C 55.96, H 4.21, N 3.35; found: C 55.91, H 4.27, N 3.30.

Synthesis of [Pd(η^3-2-Me-C_3H_4)(4-$PPh_2C_6F_4$py)$_2$](CF_3SO_3) (L^{2}c): Solid [Pd(η^3-2-Me-C_3H_4)(cod)](CF_3SO_3) (50 mg, 0.12 mmol) was added to a solution of 4-$PPh_2C_6F_4$py (100 mg, 0.24 mmol) in dichloromethane (20 mL) at room temperature. After 15 min of stirring, the reaction mixture was filtered, concentrated to 5 mL under vacuum and precipitated with diethyl ether. A pale yellow solid was obtained in 60% yield (81 mg). ^1H NMR (298 K, $CDCl_3$): δ = 8.71 (s br, 4H; $H_{\alpha\text{-py}}$), 7.48–7.42 (m, 32H; Ph, $H_{\beta\text{-py}}$), 4.06 (s br, 2H; Me-C_3H_4), 3.69 (s br, 2H; Me-C_3H_4), 1.89 ppm (s, 3H; *Me*-C_3H_4); $^{31}P\{^1H\}$ NMR (298 K, $CDCl_3$): δ = 6.3 ppm (s); ^{19}F NMR (298 K, $CDCl_3$): δ = −78.3 (s, 6F; CF_3SO_3), −125.0– −125.2 (m, 8F; F_x), −139.0– −139.5 ppm (m, 8F; F_A); IR (KBr): $\tilde{\nu}$ = 1615, 1464, 1437, 1263, 1154, 1031 cm^{-1}; ESI(+): m/z: 983.1 $[M-CF_3SO_3]^+$; calcd: 983.1; elemental analysis calcd. (%) for $C_{51}H_{35}F_{11}N_2O_3P_2PdS$: C 54.05, H 3.11, N 2.47; found: C 53.91, H 3.17, N 2.37.

Synthesis of [Pd(dppp)(4-PPh_2py)$_2$](CF_3SO_3)$_2$ (1aL^1): Solid 4-PPh_2py (30 mg, 0.11 mmol) was added to a solution of [$Pd(H_2O)_2$-(dppp)](CF_3SO_3)$_2$ (**1a**) (43 mg, 0.05 mmol) in dichloromethane (15 mL) at room temperature. After 30 min of stirring, the reaction mixture was concentrated to 5 mL under vacuum and precipitated with diethyl ether. A creamy solid was obtained in 80% yield (59 mg). ^1H NMR (298 K, $CDCl_3$): δ = 8.76 (d, J(H,H) = 4.7 Hz, 4H; $H_{\alpha\text{-py}}$), 7.61 (s br, 8H; Ph_{dppp}), 7.44–7.34 (m, 24H; Ph_{dppp}, $Ph_{4\text{-}PPh_2py}$), 7.21–7.17 (m, 8H; $Ph_{4\text{-}PPh_2py}$), 6.77 (t, J(H,H) = 4.9 Hz, 4H; $H_{\beta\text{-py}}$), 3.14 (s br, 4H; P-CH_2-), 2.30–2.17 ppm (m, 2H; C-CH_2-C); $^{31}P\{^1H\}$ NMR (298 K, $CDCl_3$): δ = 5.4 (s, dppp), −4.4 ppm (s, 4-PPh_2py); IR (KBr): $\tilde{\nu}$ = 1482,

1436, 1253, 1157, 1100, 1029 cm^{-1}; ESI(+): *m/z*: 522.1 $[M-2(CF_3SO_3)]^{2+}$; calcd: 522.1; elemental analysis calcd (%) for $C_{63}H_{54}F_6N_2O_6P_4PdS_2$: C 56.32, H 4.05, N 2.08. Found: C 56.46, H 4.07, N 2.12.

Synthesis of [Pt(dppp)(4-PPh$_2$py)$_2$](CF$_3$SO$_3$)$_2$ (1bL^1): Solid 4-PPh_2py (30 mg, 0.11 mmol) was added to a solution of $[Pt(H_2O)_2(dppp)](CF_3SO_3)_2$ (**1b**) (47 mg, 0.05 mmol) in dichloromethane (15 mL) at room temperature. After 30 min of stirring, the reaction mixture was concentrated to 5 mL under vacuum and precipitated with diethyl ether. A white solid was obtained in 85% yield (67 mg). ^{1}H NMR (298 K, $CDCl_3$): $\delta = 8.79$ (d, J(H,H) = 5.9 Hz, 4H; $H_{\alpha\text{-py}}$), 7.63 (s br, 8H; Ph_{dppp}), 7.45–7.35 (m, 24H; Ph_{dppp}, $Ph_{4\text{-}PPh_2py}$), 7.22–7.18 (m, 8H; $Ph_{4\text{-}PPh_2py}$), 6.80 (t, J(H,H) = 5.4 Hz, 4H; $H_{\beta\text{-py}}$), 3.24 (s br, 4H; P-CH_2-), 2.27–2.17 ppm (m, 2H; C-CH_2-C); ^{31}P{^{1}H} NMR (298 K, $CDCl_3$): $\delta = -3.8$ (s, 4-PPh_2py), −16.0 (s, ^1J(Pt,P) = 3051 Hz, dppp); IR (KBr): $\tilde{\nu} = 1481$, 1438, 1256, 1153, 1100, 1031 cm^{-1}; ESI(+): *m/z*: 1282.2 $[M-CF_3SO_3]^+$; calcd: 1283.2; 566.6 $[M-2(CF_3SO_3)]^{2+}$; calcd: 566.6; elemental analysis calcd (%) for $C_{63}H_{54}F_6N_2O_6P_4PtS_2$: C 52.83, H 3.80, N 1.96; found: C 52.96, H 3.78, N 1.95.

Self-assembly of [{Pd(η^3-2-Me-C$_3$H$_4$)(4-PPh$_2$py)$_2$}$_2${Pd(PPh$_3$)$_2$}$_2$](CF$_3$SO$_3$)$_6$ (2aL^{1}c)

Method 1: A solution of $[Pd(\eta^3\text{-2-Me-}C_3H_4)(cod)](CF_3SO_3)$ (25 mg, 0.06 mmol) and 4-PPh_2py (31 mg, 0.12 mmol) in dichloromethane (10 mL) was added to a solution of $[Pd(H_2O)_2(PPh_3)_2](CF_3SO_3)_2$ (**2a**) (58 mg, 0.06 mmol) in dichloromethane (5 mL) at room temperature. After 30 min of stirring, the reaction mixture was filtered, concentrated to 5 mL under vacuum and precipitated with diethyl ether. A white solid was obtained in 75% yield (79 mg).

Method 2: A solution of $[Pd(\eta^3\text{-2-Me-}C_3H_4)(4\text{-}PPh_2py)_2](CF_3SO_3)$ (**L^{1}c**) (50 mg, 0.06 mmol) in dichloromethane (10 mL) was added dropwise to a solution of $[Pd(H_2O)_2(PPh_3)_2](CF_3SO_3)_2$ (**2a**) (58 mg, 0.06 mmol) in dichloromethane (5 mL) at room temperature. After 30 min of stirring the solution was concentrated to 5 mL under vacuum and precipitated with diethyl ether. A white solid was obtained in 80% yield (85 mg).

^{1}H NMR (298 K, [D$_6$]acetone): $\delta = 9.14$ (d, J(H,H) = 8.0 Hz, 8H; $H_{\alpha\text{-py}}$), 7.76–6.98 (m, 108H; Ph, $H_{\beta\text{-py}}$), 3.87 (s, 4H; Me-C_3H_4), 2.29–2.26 (m, 4H; Me-C_3H_4), 1.94 ppm (s, 6H; *Me*-C_3H_4); ^{31}P{^{1}H} NMR (298 K, [D$_6$]acetone): $\delta = 26.6$ (s, PPh_2py), 26.3 ppm (s, PPh_3); IR (KBr): $\tilde{\nu} =$ 1616, 1480, 1438, 1256, 1153, 1030 cm^{-1}; ESI(+): *m/z*: 2192.2 $[Pd_3(\eta^3\text{-2-Me-}C_3H_4)_2(PPh_3)_2(4\text{-}PPh_2py)_3(CF_3SO_3)_3]^+$; calcd: 2191.1); 1617.2 [**2aL^{1}c**−2(CF$_3$SO$_3$)]$^{2+}$, $[Pd_2(\eta^3\text{-2-Me-}C_3H_4)(PPh_3)_2(4\text{-}PPh_2py)_2(CF_3SO_3)_2]^+$; calcd: 1617.1; 1354.1 $[Pd_2(\eta^3\text{-2-Me-}C_3H_4)(PPh_3)_2(4\text{-}PPh_2py)(CF_3SO_3)_2]^+$; calcd: 1354.0; 1198.6 $[Pd_3(\eta^3\text{-2-Me-}C_3H_4)(PPh_3)_4(4\text{-}PPh_2py)_2(CF_3SO_3)_3]^{2+}$; calcd: 1198.6; 779.1 $[Pd(PPh_3)_2(CF_3SO_3)]^+$; calcd: 779.0) 685.2 $[Pd(\eta^3\text{-2-Me-}C_3H_4)(PPh_3)_2]^+$, $[Pd(\eta^3\text{-2-Me-}C_3H_4)(PPh_3)(4\text{-}PPh_2py)]^+$, $[Pd(\eta^3\text{-2-Me-}C_3H_4)(4\text{-}PPh_2py)_2]^+$; calcd: 685.1, 686.1, 687.1.

Self-assembly of [{Pd(η^3-2-Me-C$_3$H$_4$)(4-PPh$_2$py)$_2$}$_2${Pt(PPh$_3$)$_2$}$_2$](CF$_3$SO$_3$)$_6$ (2bL^{1}c): A solution of $[Pd(\eta^3\text{-2-Me-}C_3H_4)(4\text{-}PPh_2py)_2](CF_3SO_3)$ (**L^{1}c**) (50 mg, 0.06 mmol) in dichloromethane (15 mL) was added to a solution of $[PtCl_2(PPh_3)_2]$ (47 mg, 0.06 mmol) in dichloromethane (15 mL) at room temperature. After a few minutes of stirring $AgCF_3SO_3$ (31 mg, 0.12 mmol) was added and the reaction mixture was stirred for two hours at room temperature light protected. Then the solution was filtered through celite, concentrated to 5 mL under vacuum and precipitated with diethyl ether. A yellowish solid was obtained in 86% yield (95 mg). ^{1}H NMR (298 K, [D$_6$]acetone): $\delta = 9.18$ (d, J(H,H) = 6.0 Hz, 8H; $H_{\alpha\text{-py}}$), 7.77–7.05 (m, 108H; Ph, $H_{\beta\text{-py}}$), 3.93 (s, 4H; Me-C_3H_4), 2.29–2.26 (m, 4H; Me-C_3H_4), 1.95 ppm (s, 6H; *Me*-C_3H_4); ^{1}H NMR (220 K, $CDCl_3$): $\delta =$ 9.31 (s, 4H; $H_{\alpha\text{-py}}$), 8.76 (s, 4H; $H_{\alpha\text{-py}}$), 7.68–7.29 (m, 60H; Ph), 7.19–6.80 (m, 48H; Ph, $H_{\beta\text{-py}}$), 3.50 (s, 4H; Me-C_3H_4), 2.23 (s, 4H; Me-C_3H_4), 1.78 ppm (s, 6H; *Me*-C_3H_4); ^{31}P{^{1}H} NMR (298 K, [D$_6$]acetone): $\delta = 26.6$ (s, PPh_2py), 0.6 ppm (s, ^1J(Pt,P) = 3323 Hz, PPh_3); IR (KBr): $\tilde{\nu} = 1616$, 1470, 1438, 1258, 1157, 1031 cm^{-1}; ESI(+): *m/z*: 2324.3 [(**2bL^1**)$_2$−3(CF$_3$SO$_3$)]$^{3+}$; calcd: 2324.3; 2280.2 $[PtPd_2(\eta^3\text{-2-Me-}C_3H_4)_2(PPh_3)_2(4\text{-}PPh_2py)_3(CF_3SO_3)_3]^+$; calcd: 2279.2; 1706.2 [**2bL^{1}c**−2(CF$_3$SO$_3$)]$^{2+}$, $[PtPd(\eta^3\text{-2-Me-}C_3H_4)(PPh_3)_2(4\text{-}PPh_2py)_2(CF_3SO_3)_2]^+$; calcd: 1705.7; 1442.1 $[PtPd(\eta^3\text{-2-Me-}C_3H_4)(PPh_3)_2(4\text{-}PPh_2py)(CF_3SO_3)_2]^+$; calcd: 1442.1; 1131.2 $[Pt(PPh_3)_2(4\text{-}PPh_2py)(CF_3SO_3)]^+$; calcd: 1131.2; 1087.5 [**2bL^{1}c**−3(CF$_3$SO$_3$)]$^{3+}$; calcd: 1087.5); 1065.1 $[PtPd_2(\eta^3\text{-2-Me-}C_3H_4)_2(PPh_3)_2(4\text{-}PPh_2py)_3(CF_3SO_3)_2]^{2+}$; calcd: 1065.1; 687.1 $[Pd(\eta^3\text{-2-Me-}C_3H_4)(4\text{-}PPh_2py)_2]^+$; calcd: 687.1.

Self-assembly of [{Pd(η^3-2-Me-C$_3$H$_4$)(4-PPh$_2$C$_6$F$_4$py)$_2$}$_2${Pd(dppp)}$_2$](CF$_3$SO$_3$)$_6$ (1aL^{2}c): A solution of $[Pd(\eta^3\text{-2-Me-}C_3H_4)(cod)](CF_3SO_3)$ (10 mg, 0.02 mmol) in dichloromethane (5 mL) was added to a solution of $[Pd(H_2O)_2(dppp)](CF_3SO_3)_2$ (**1a**) (20 mg, 0.02 mmol) in dichloromethane (5 mL) at room temperature and then a solution of 4-$PPh_2C_6F_4py$ (20 mg, 0.05 mmol) in dichloromethane (5 mL) was added to this mixture. After 30 min. of stirring, the reaction mixture was filtered, concentrated to 5 mL under vacuum and precipitated with diethyl ether. A yellow solid was obtained in 75% yield (36 mg). ^{1}H NMR (298 K, [D$_6$]acetone): $\delta = 9.23$ (d, J(H,H) = 5.0 Hz, 8H; $H_{\alpha\text{-py}}$), 7.85–7.33 (m, 88H; $H_{\beta\text{-py}}$, Ph), 4.17 (d, J(H,P) = 7.5 Hz, 4H; Me-C_3H_4), 3.73–3.68 (m, 4H; Me-C_3H_4), 3.43 (s br, 8H; P-CH_2-), 2.53–2.33 (m, 4H; C-CH_2-C), 1.94 (s, 3H; *Me*-C_3H_4), 1.92 ppm (s, 3H; *Me*-C_3H_4); ^{31}P{^{1}H} NMR (298 K, [D$_6$]acetone): $\delta = 9.2$ (s br, 4-$PPh_2C_6F_4py$), 8.0 ppm (s, dppp); ^{19}F NMR (298 K, [D$_6$]acetone): $\delta = -78.1$ (s, 6F; CF_3SO_3), −124.5 (s br, 8F; F_x), −139.1– −139.2 ppm (m, 8F; F_A); IR (KBr): $\tilde{\nu} = 1616$, 1464, 1437, 1259, 1158, 1030 cm^{-1}; ESI(+): *m/z* = 1801.1 [(**1aL^{2}c**−2(CF$_3$SO$_3$)]$^{2+}$; calcd: 1801.1; 1295.0 $[Pd_2(\eta^3\text{-2-Me-}C_3H_4)_2(4\text{-}PPh_2C_6F_4py)_2(CF_3SO_3)]^+$; calcd: 1295.0; 1234.5 $[Pd_3(\eta^3\text{-2-Me-}C_3H_4)_2(dppp)_2(4\text{-}PPh_2C_6F_4py)_2(CF_3SO_3)_3]^{2+}$; calcd: 1234.0); 1187.0 $[Pd_3(\eta^3\text{-2-Me-}C_3H_4)_2(dppp)(4\text{-}PPh_2C_6F_4py)_3(CF_3SO_3)_2]^{2+}$: calcd: 1186.6; 1151.1 [**1aL^{2}c**−3(CF$_3$SO$_3$)]$^{3+}$; calcd: 1151.1; 983.1 $[Pd(\eta^3\text{-2-Me-}C_3H_4)(4\text{-}PPh_2C_6F_4py)_2]^+$; calcd: 983.1; 667.0 $[Pd(dppp)(CF_3SO_3)]^+$; calcd: 667.0; 572.5 $[Pd_2(\eta^3\text{-2-Me-}C_3H_4)_2(4\text{-}PPh_2C_6F_4py)_2]^{2+}$; calcd: 573.0.

Self-assembly of [{Pd(η^3-2-Me-C$_3$H$_4$)(4-PPh$_2$C$_6$F$_4$py)$_2$}$_2${Pt(dppp)}$_2$](CF$_3$SO$_3$)$_6$ (1bL^{2}c): A solution of $[Pd(\eta^3\text{-2-Me-}C_3H_4)(cod)](CF_3SO_3)$ (10 mg, 0.02 mmol) in dichloromethane (5 mL) was added to a solution of $[Pt(H_2O)_2(dppp)](CF_3SO_3)_2$ (**1b**) (23 mg, 0.02 mmol) in dichloromethane (5 mL) at room temperature and then a solution of 4-$Ph_2C_6F_4py$ (20 mg, 0.05 mmol) in dichloromethane (5 mL) was added to this mixture. After 30 min. of stirring, the reaction mixture was filtered, concentrated to 5 mL under vacuum and precipitated with diethyl ether. A yellow solid was obtained in 70% yield (34 mg). ^{1}H NMR (298 K, [D$_6$]acetone): $\delta = 9.26$ (d, J(H-H) = 6.0 Hz, 8H; $H_{\alpha\text{-py}}$), 7.89–7.36 (m, 88H, $H_{\beta\text{-py}}$, Ph), 4.18 (d, J(H,P) = 10.0 Hz, 4H; Me-C_3H_4), 3.73–3.68 (m, 4H; Me-C_3H_4), 3.52 (s br, 8H; P-CH_2), 2.50–2.26 (m, 4H; C-CH_2-C), 1.94 (s, 3H; *Me*-C_3H_4), 1.92 ppm (s, 3H; *Me*-C_3H_4); ^{31}P{^{1}H} NMR (298 K, [D$_6$]acetone: $\delta = 9.4$ (s br, 4-$PPh_2C_6F_4py$), −14.2 ppm (s, ^1J(P,Pt) = 3055 Hz, dppp); ^{19}F NMR (298 K, [D$_6$]acetone): $\delta = -78.7$ (s, 6F; CF_3SO_3), −126.7 (s br, 8F; F_x), −141.0– −141.1 ppm (m, 8F; F_A); IR (KBr): $\tilde{\nu} = 1617$, 1468, 1437, 1259, 1158, 1031 cm^{-1}; ESI(+): *m/z*: 1890.1 [**1bL^{2}c**−2(CF$_3$SO$_3$)]$^{2+}$; calcd: 1890.1; 1295.0 $[Pd_2(\eta^3\text{-2-Me-}C_3H_4)_2(4\text{-}PPh_2C_6F_4py)_2(CF_3SO_3)]^+$; calcd: 1295.0; 1210.1 [**1bL^{2}c**−3(CF$_3$SO$_3$)]$^{3+}$; calcd: 1210.1; 870.1 [**1bL^{2}c**−4(CF$_3$SO$_3$)]$^{4+}$; calcd: 870.3; 573.0 $[Pd_2(\eta^3\text{-2-Me-}C_3H_4)_2(4\text{-}PPh_2C_6F_4py)_2]^+$; calcd: 573.0.

Acknowledgments

Financial support for this work was provided by the Ministerio de Economía y Competitividad (MINECO/FEDER) of Spain (Projects CTQ2012-31335, CTQ2012-37821-C02-01 and CT2010-15292/BQU), and of the Deutsche Forschungsgemeinschaft (SFB 624).

Keywords: allyl ligands · homogeneous catalysis · kinetico-mechanistic studies · metallamacrocycles · self-assembly

[1] a) G. F. Swiegers, T. J. Malefetse, *Chem. Rev.* **2000**, *100*, 3483 – 3537; b) L. Cronin, *Annu. Rep. Prog. Chem., Sect. A: Inorg. Chem.* **2004**, *100*, 323 – 383; c) C. L. Chen, J. Y. Zhang, C. Y. Su, *Eur. J. Inorg. Chem.* **2007**, 2997 – 3010; d) E. C. Constable, *Coord. Chem. Rev.* **2008**, *252*, 842 – 855; e) M. W. Cooke, D. Chartrand, G. S. Hanan, *Coord. Chem. Rev.* **2008**, *252*, 903 – 921; f) A. Kumar, S. S. Sun, A. J. Lees, *Coord. Chem. Rev.* **2008**, *252*, 922 – 939; g) B. H. Northrop, H. B. Yang, P. J. Stang, *Chem. Commun.* **2008**, 5896 – 5908; h) E. Zangrando, M. Casanova, E. Alessio, *Chem. Rev.* **2008**, *108*, 4979 – 5013; i) B. H. Northrop, Y. R. Zheng, K. W. Chi, P. J. Stang, *Acc. Chem. Res.* **2009**, *42*, 1554 – 1563; j) R. Chakrabarty, P. S. Mukherjee, P. J. Stang, *Chem. Rev.* **2011**, *111*, 6810 – 6918; k) H. Amouri, C. Desmarets, J. Moussa, *Chem. Rev.* **2012**, *112*, 2015 – 2041; l) T. R. Cook, Y. R. Zheng, P. J. Stang, *Chem. Rev.* **2013**, *113*, 734 – 777.

[2] a) C. A. Schalley, A. Lutzen, M. Albrecht, *Chem. Eur. J.* **2004**, *10*, 1072 – 1080; b) F. Wurthner, C. C. You, C. R. Saha-Moller, *Chem. Soc. Rev.* **2004**, *33*, 133 – 146; c) C. H. M. Amijs, G. P. M. van Klink, G. van Koten, *Dalton Trans.* **2006**, 308 – 327; d) S. J. Lee, W. B. Lin, *Acc. Chem. Res.* **2008**, *41*, 521 – 537; e) J. W. Steed, *Chem. Soc. Rev.* **2009**, *38*, 506 – 519.

[3] a) K. Takaoka, M. Kawano, T. Ozeki, M. Fujita, *Chem. Commun.* **2006**, 1625 – 1627; b) M. Yoshizawa, J. K. Klosterman, M. Fujita, *Angew. Chem.* **2009**, *121*, 3470 – 3490; *Angew. Chem. Int. Ed.* **2009**, *48*, 3418 – 3438; c) J. L. Hou, D. Ajami, J. Rebek, *J. Am. Chem. Soc.* **2008**, *130*, 7810 – 7811; d) M. D. Pluth, R. G. Bergman, K. N. Raymond, *Acc. Chem. Res.* **2009**, *42*, 1650 – 1659; e) D. Fiedler, D. H. Leung, R. G. Bergman, K. N. Raymond, *Acc. Chem. Res.* **2005**, *38*, 349 – 358; f) T. H. Noh, E. Heo, K. H. Park, O. S. Jung, *J. Am. Chem. Soc.* **2011**, *133*, 1236 – 1239.

[4] a) H. Jiang, A. Hu, W. Lin, *Chem. Commun.* **2003**, 96 – 97; b) H. Wang, R. Zhong, X. Q. Guo, X. Y. Feng, X. F. Hou, *Eur. J. Inorg. Chem.* **2010**, 174 – 178; c) J. Park, S. Hong, *Chem. Soc. Rev.* **2012**, *41*, 6931 – 6943.

[5] I. Angurell, M. Ferrer, A. Gutierrez, M. Martinez, L. Rodriguez, O. Rossell, M. Engeser, *Chem. Eur. J.* **2010**, *16*, 13960 – 13964.

[6] H. Tsuji, *Palladium Reagents and Catalysis*, Wiley, New York, **2004**.

[7] a) B. M. Trost, D. L. Van Vranken, *Chem. Rev.* **1996**, *96*, 395 – 422; b) B. M. Trost, C. Lee in *Catalytic Asymmetric Synthesis* (Ed.: I. Ojima), Wiley-VCH, Weinheim, **2000**; c) L. Milhan, P. J. Guiry in *Transition-Metal-Catalysed Enantioselective Allylic Substitution in Organic Synthesis* (Ed.: U. Kazmaier), Springer, Heidelberg, **2012**.

[8] a) T. V. Rajan Babu, *Chem. Rev.* **2003**, *103*, 2845 – 2860; b) R. M. Ceder, A. Grabulosa, G. Muller, M. Rocamora, *Catal. Sci. Technol.* **2013**, *3*, 1446 – 1464.

[9] a) S. J. Park, D. M. Shin, S. Sakamoto, K. Yamaguchi, Y. K. Chung, M. S. Lah, J. Hong, *Chem. Eur. J.* **2005**, *11*, 235 – 241; b) D. C. Caskey, T. Yamamoto, C. Addicott, R. K. Shoemaker, J. Vacek, A. M. Hawkridge, D. C. Muddiman, G. S. Kottas, J. Michl, P. J. Stang, *J. Am. Chem. Soc.* **2008**, *130*, 7620 – 7628; c) J. Vacek, D. C. Caskey, D. Horinek, R. K. Shoemaker, P. J. Stang, J. Michl, *J. Am. Chem. Soc.* **2008**, *130*, 7629 – 7638; d) Y. R. Zheng, P. J. Stang, *J. Am. Chem. Soc.* **2009**, *131*, 3487 – 3489; e) A. Gonzalez-Alvarez, A. Frontera, P. Ballester, *J. Phys. Chem. B* **2009**, *113*, 11479 – 11489.

[10] a) G. Tarkanyi, H. Jude, G. Palinkas, P. J. Stang, *Org. Lett.* **2005**, *7*, 4971 – 4973; b) M. Fuss, H. U. Siehl, B. Olenyuk, P. J. Stang, *Organometallics* **1999**, *18*, 758 – 769.

[11] M. Ferrer, M. Mounir, O. Rossell, E. Ruiz, M. A. Maestro, *Inorg. Chem.* **2003**, *42*, 5890 – 5899.

[12] a) B. Brusilowskij, E. V. Dzyuba, R. W. Troff, C. A. Schalley, *Dalton Trans.* **2011**, *40*, 12089 – 12096; b) M. L. Tobe, J. Burgess, *Inorganic Reaction Mechanisms*, Longman, New York, **1999**.

[13] a) C. A. Schalley, T. Muller, P. Linnartz, M. Witt, M. Schafer, A. Lutzen, *Chem. Eur. J.* **2002**, *8*, 3538 – 3551; b) M. Ferrer, A. Gutierrez, L. Rodriguez, O. Rossell, E. Ruiz, M. Engeser, Y. Lorenz, R. Schilling, P. Gomez-Sal, A. Martin, *Organometallics* **2012**, *31*, 1533 – 1545.

[14] a) K. S. Jeong, S. Y. Kim, U. S. Shin, M. Kogej, N. T. M. Hai, P. Broekmann, N. Jeong, B. Kirchner, M. Reiher, C. A. Schalley, *J. Am. Chem. Soc.* **2005**, *127*, 17672 – 17685; b) M. Ferrer, A. Pedrosa, L. Rodriguez, O. Rossell, M. Vilaseca, *Inorg. Chem.* **2010**, *49*, 9438 – 9449; c) T. Weilandt, N. L. Low, G. Schnakenburg, J. Daniels, M. Nieger, C. A. Schalley, A. Lutzen, *Chem. Eur. J.* **2012**, *18*, 16665 – 16676; d) M. Ferrer, A. Gutierrez, M. Mounir, O. Rossell, E. Ruiz, A. Rang, M. Engeser, *Inorg. Chem.* **2007**, *46*, 3395 – 3406.

[15] Alternatively, the formation of the metallamacrocycles can also be achieved in good yields from the self-assembly of the building blocks indicated in Scheme 3, bottom.

[16] a) C. A. Schalley, *Mass Spectrom. Rev.* **2001**, *20*, 253 – 309; b) B. Baytekin, H. T. Baytekin, C. A. Schalley, *Org. Biomol. Chem.* **2006**, *4*, 2825 – 2841; c) M. Kogej, C. A. Schalley, *Analytical Methods in Supramolecular Chemistry* (Ed.: C. A. Schalley), Wiley-VCH, Weinheim, **2007**; d) C. A. Schalley, A. Springer, *Mass Spectrometry and Gas Phase Chemistry of Non-Covalent Complexes*, Wiley, New York, **2009**; e) L. Cera, C. A. Schalley, *Chem. Soc. Rev.* **2014**, *43*, 1800 – 1812.

[17] a) C. G. Claessens, M. J. Vicente-Arana, T. Torres, *Chem. Commun.* **2008**, 6378 – 6380; b) V. M. Cangelosi, T. G. Carter, L. N. Zakharov, D. W. Johnson, *Chem. Commun.* **2009**, 5606 – 5608; c) Y. R. Zheng, H. B. Yang, K. Ghosh, L. Zhao, P. J. Stang, *Chem. Eur. J.* **2009**, *15*, 7203 – 7214; d) J. S. Mathieson, G. J. T. Cooper, A. L. Pickering, M. Keller, D. L. Long, G. N. Newton, L. Cronin, *Chem. Asian J.* **2009**, *4*, 681 – 687; e) S. Sato, Y. Ishido, M. Fujita, *J. Am. Chem. Soc.* **2009**, *131*, 6064 – 6065; f) B. R. Hall, L. E. Manck, I. S. Tidmarsh, A. Stephenson, B. F. Taylor, E. J. Blaikie, D. A. Vander Griend, M. D. Ward, *Dalton Trans.* **2011**, *40*, 12132 – 12145; g) W. Jiang, A. Schafer, P. C. Mohr, C. A. Schalley, *J. Am. Chem. Soc.* **2010**, *132*, 2309 – 2320.

[18] a) D. Fujita, A. Takahashi, S. Sato, M. Fujita, *J. Am. Chem. Soc.* **2011**, *133*, 13317 – 13319; b) S. J. Li, J. Y. Huang, T. R. Cook, J. B. Pollock, H. Kim, K. W. Chi, P. J. Stang, *J. Am. Chem. Soc.* **2013**, *135*, 2084 – 2087.

[19] gNMR version 5.0, P. H. H. Budzelaar, Cherwell Scientific, **1995**.

[20] a) E. S. Barrett, T. J. Dale, J. Rebek, *J. Am. Chem. Soc.* **2007**, *129*, 8818 – 8824; b) A. V. Davis, D. Fiedler, M. Ziegler, A. Terpin, K. N. Raymond, *J. Am. Chem. Soc.* **2007**, *129*, 15354 – 15363.

[21] C. Reichardt, *Solvents and Solvent Effects in Organic Chemistry*, 3edth ed-Wiley-VCH, Weinheim, **2003**.

[22] A. G. Lappin, *Redox Mechanisms in Inorganic Chemistry*, Elis Horwood, New York, **1994**.

[23] a) T. Hayashi, M. Kawatsura, Y. Uozumi, *J. Am. Chem. Soc.* **1998**, *120*, 1681 – 1687; b) R. J. van Haaren, P. H. Keeven, L. A. van der Veen, K. Goubitz, G. P. F. van Strijdonck, H. Oevering, J. N. H. Reek, P. C. J. Kamer, P. W. N. M. van Leeuwen, *Inorg. Chim. Acta* **2002**, *327*, 108 – 115.

[24] a) R. J. van Haaren, C. J. M. Druijven, G. P. F. van Strijdonck, H. Oevering, J. N. H. Reek, P. C. J. Kamer, P. W. N. M. van Leeuwen, *J. Chem. Soc. Dalton Trans.* **2000**, 1549 – 1554; b) M. D. K. Boele, P. C. J. Kamer, M. Lutz, A. L. Spek, J. G. de Vries, P. W. N. M. van Leeuwen, G. P. E. van Strijdonck, *Chem. Eur. J.* **2004**, *10*, 6232 – 6246; c) S. C. Milheiro, J. W. Faller, *J. Organomet. Chem.* **2011**, *696*, 879 – 886.

[25] a) V. F. Slagt, M. Roder, P. C. J. Kamer, P. W. N. M. van Leeuwen, J. N. H. Reek, *J. Am. Chem. Soc.* **2004**, *126*, 4056 – 4057; b) V. F. Slagt, P. W. N. M. van Leeuwen, J. N. H. Reek, *Dalton Trans.* **2007**, 2302 – 2310; c) P. E. Goudriaan, X. B. Jang, M. Kuil, R. Lemmens, P. W. N. M. Van Leeuwen, J. N. H. Reek, *Eur. J. Org. Chem.* **2008**, 6079 – 6092.

[26] C. J. Kuehl, S. D. Huang, P. J. Stang, *J. Am. Chem. Soc.* **2001**, *123*, 9634 – 9641.

[27] M. Fujita, F. Ibukuro, K. Yamaguchi, K. Ogura, *J. Am. Chem. Soc.* **1995**, *117*, 4175 – 4176.

[28] a) U. Frey, L. Helm, A. E. Merbach, R. Romeo, *J. Am. Chem. Soc.* **1989**, *111*, 8161 – 8165; b) G. Alibrandi, G. Bruno, S. Lanza, D. Minniti, R. Romeo, M. L. Tobe, *Inorg. Chem.* **1987**, *26*, 185 – 190; c) G. Alibrandi, D. Minniti, L. M. Scolaro, R. Romeo, *Inorg. Chem.* **1989**, *28*, 1939 – 1943; d) M. R. Plutino, L. M. Scolaro, A. Albinati, R. Romeo, *J. Am. Chem. Soc.* **2004**, *126*, 6470 – 6484.

[29] a) R. van Eldik, *Advances in Inorganic Chemistry, Vol. 59*, Academic Press, New York, **2006**; b) S. Hochreuther, S. T. Nandibewoor, R. Puchta, R. van Eldik, *Dalton Trans.* **2012**, *41*, 512 – 522; c) T. Soldatovic, S. Jovanovic, Z. D. Bugarcic, R. van Eldik, *Dalton Trans.* **2012**, *41*, 876 – 884.
[30] a) G. R. Newkome, D. C. Hager, *J. Org. Chem.* **1978**, *43*, 947 – 949; b) L. Hirsivaara, M. Haukka, J. Pursiainen, *J. Organomet. Chem.* **2001**, *633*, 66 – 68.
[31] P. J. Stang, D. H. Cao, S. Saito, A. M. Arif, *J. Am. Chem. Soc.* **1995**, *117*, 6273 – 6283.
[32] F. Dejong, J. J. Bour, P. P. J. Schlebos, *Inorg. Chim. Acta* **1988**, *154*, 89 – 93.
[33] Z. Qin, M. C. Jennings, R. J. Puddephatt, *Inorg. Chem.* **2001**, *40*, 6220 – 6228.
[34] W. T. Dent, R. Long, A. J. Wilkinson, *J. Chem. Soc.* **1964**, 1585 – 1588.
[35] D. A. White, J. R. Doyle, H. Lewis in *Inorg. Synth., Vol. 13* (Ed.: F. A. Cotton), Wiley, Hoboken, **1972**, pp. 55 – 62.

Received: May 9, 2014
Published online on ■■ ■■, 0000

FULL PAPER

Self-Assembly

I. Angurell, M. Ferrer, A. Gutiérrez, M. Martínez,* M. Rocamora, L. Rodríguez, O. Rossell, Y. Lorenz, M. Engeser*

■■ – ■■

Kinetico-Mechanistic Insights on the Assembling Dynamics of Allyl-Cornered Metallacycles: The Pt–N_{py} Bond is the Keystone

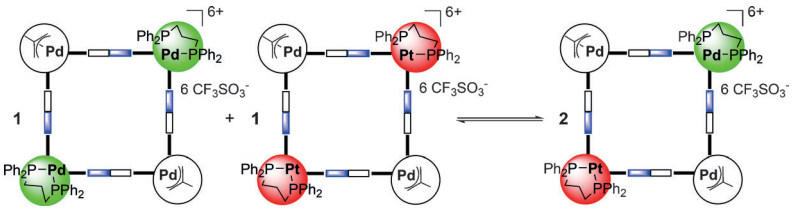

Platinum is the winner! Pt–N_{py} bonds play a keystone role in the kinetics of formation and solution behaviour of several homo- and heterometallomacrocycles containing allyl-palladium corners. The exchange among different combinations of adequate building blocks and the supramolecular species has been studied, and a preliminary study of the role of theses assemblies as catalysts in the allylic alkylation reaction has been undertaken.